

AlignBench: Benchmarking Fine-Grained Image-Text Alignment with Synthetic Image-Caption Pairs

Kuniaki Saito^{1*}, Risa Shinoda^{2*}, Shohei Tanaka¹, Toshio Hirasawa¹, Fumio Okura², Yoshitaka Ushiku¹
¹OMRON SINIC X Corporation ²The University of Osaka

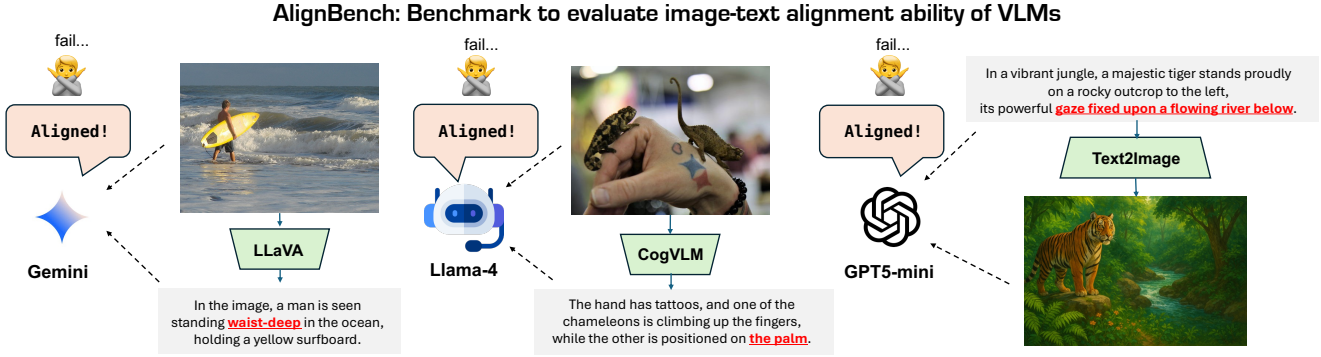


Figure 1. We introduce a novel benchmark, **AlignBench**, which evaluates the VLM’s ability for text-image alignment. We employ state-of-the-art Image-to-Text and Text-to-Image models to create synthetic image-caption pairs with or without subtle hallucinations. Misaligned words are highlighted in red. Using this dataset, we benchmark diverse VLMs to assess their ability to understand the alignment of image-sentence pairs. We find that subtle hallucinations generated by multimodal models can be hard to detect, even by state-of-the-art VLMs.

Abstract

Assessing image-text alignment models such as CLIP is crucial for bridging visual and linguistic representations. Yet existing benchmarks rely on rule-based perturbations or short captions, limiting their ability to measure fine-grained alignment. We introduce AlignBench, a benchmark that provides a new indicator of image-text alignment by evaluating detailed image-caption pairs generated by diverse image-to-text and text-to-image models. Each sentence is annotated for correctness, enabling direct assessment of VLMs as alignment evaluators. Benchmarking a wide range of decoder-based VLMs reveals three key findings: (i) CLIP-based models, even those tailored for compositional reasoning, remain nearly blind; (ii) detectors systematically over-score early sentences; and (iii) they show strong self-preference, favoring their own outputs and harming detection performance. Our project page will be available at <https://dahlian00.github.io/AlignBench/>.

1. Introduction

Image-text alignment models, such as CLIP [42], play an essential role in bridging visual and linguistic representations. These models have the potential to enhance the performance on diverse downstream tasks, including classification [64], captioning [4], dataset curation [28], and even in 3D scene understanding [9]. While recent studies suggest that CLIP has limited ability to measure fine-grained alignment between images and texts [22, 40, 48, 61], large vision-language models (VLMs) are expected as promising alternatives since they exhibit strong multimodal reasoning and generation capabilities [7, 29, 32, 33, 53].

As the importance of VLMs increases, evaluating the ability of image-text alignment models becomes crucial. However, existing benchmarks [22, 61] for evaluating image-text alignment often rely on rule-based caption perturbations, such as replacing words with semantically related or unrelated terms or simple captions [48], which are not suitable for evaluating fine-grained alignment.

As a foundation for the future development of image-text alignment models, we propose a new benchmark, *AlignBench*, designed to evaluate fine-grained image-text alignment. Unlike existing benchmarks relying on

*Equal contribution. Kuniaki serves as the project lead, while Risa is responsible for dataset construction. kuniaki.saito@sinicx.com, shinoda.risa@ist.osaka-u.ac.jp.



Figure 2. **AlignBench** spans diverse Image2Text (*i.e.*, Captioner) and Text2Image models, diverse image domains, and provides high-quality annotations enriched with hallucination-type labels for deep analysis. The rightmost figure presents the example of annotations. We first conduct sentence-level correctness annotation and further annotate the segment of hallucination and its type label.

rule-based perturbations, we provide annotations for image-captions pairs generated by VLM *Captioners*¹ and Text2Image models, indicating whether the text correctly describes the image content, and assess VLM *Evaluator* models to measure their image-text alignment performance, as illustrated in Fig. 1.

Using VLM-generated captions as evaluation targets offers two major advantages. First, VLM-generated captions can serve as *hard-negatives* for evaluators. While modern captioners can capture coarse visual content effectively, they often struggle to express fine-grained details in language, producing hallucinations—textual content inconsistent with the image. Evaluating against such mismatched image-text pairs allows us to directly assess an evaluator’s ability to judge challenging cases where achieving alignment is inherently difficult for VLMs. Second, evaluating VLM-generated captions enables direct assessment of a model’s ability to filter synthetic image-caption pairs and clean noisy multimodal datasets.

This task can be regarded as a hallucination detection in image captions, yet we highlight an important aspect of this task, *i.e.*, revealing the fundamental image-text alignment ability. Existing datasets for hallucination detection [10, 20, 58] are not suited for benchmarking the model’s ability because of the lack of model coverage and the small number of evaluation samples. Instead, as shown in Fig. 2, we aim to cover a diverse range of models with sufficient samples, which is useful for comprehensive analysis.

Our experiments focus on benchmarking diverse VLM evaluators on sentence-level alignment evaluation. Empirically, we observe that models performing well on AlignBench also achieve strong results on prior hallucination and compositionality benchmarks, whereas the reverse does not necessarily hold. This asymmetry indicates that AlignBench provides a new and more comprehensive indicator of image-text alignment ability. Our extensive analysis further yields several key insights. First, CLIP-based models, even the one tailored for compositional alignment, remain nearly blind. Second, evaluators tend

to recognize sentences at the beginning of a response as *correct*, regardless of their correctness. Third, they exhibit self-preference, *i.e.* consider their own output captions as *correct*, which degrades performance as detectors. This observation is consistent with prior findings [39].

2. Related Work

Benchmarks for VLMs. Many benchmarks evaluate the reasoning ability of VLMs [18, 19, 26, 49, 59, 60] or expert knowledge [34]. We focus on assessing their fundamental capability to understand the fine-grained image-text alignment. Tong *et al.* [50] evaluate fine-grained visual comprehension using CLIP-blind image pairs and related questions; while we propose a new task for a fine-grained benchmark, *i.e.*, AlignBench provides the task of detecting the actual errors in captions generated by advanced VLMs.

Image-caption alignment datasets. Winoground [48], SUGARCREPE [22], and ARO [61] assess CLIP’s fine-grained image-text alignment ability. All focus on compositional structure in short sentences, and SUGARCREPE and ARO rely on rule-based perturbations. In contrast, AlignBench uses VLM-generated captions that enable evaluation on more complex and natural texts. This allows us to directly assess models on cases where VLMs themselves tend to fail in understanding, which is shown to be more challenging as shown in Sec. 4.2. SeeTRUE [58] uses AI-generated image-caption pairs, but its captions are short and simple, making it unsuitable for fine-grained alignment evaluation. GenAI-Bench [31] benchmarks scoring metrics by ranking images generated from the same prompt, relying on concise captions and relative ranking rather than binary alignment labels. Some datasets are introduced for hallucination detection in image captions [10, 20, 51, 52]², but they are limited as VLM benchmarks, often lacking diverse captioners or sufficient samples per model. Our benchmark, AlignBench, addresses these gaps by (i) covering more responses, (ii) balancing data across diverse models, and (iii) incorporating text-to-image outputs. We provide a more detailed comparison in Table C of the appendix.

¹We refer to a VLM used for caption generation as a *Captioner*, and to one used for assessing image-text alignment as an *Evaluator* or *Detector*.

²ZINA [51] is concurrent with ours, and details were unavailable at the time of submission; we compare as best we can.



Captioner: GPT-4o

These stickers represent different locations such as California, New York City, and [Route 66](#), among others.



Captioner: Llama-4

The image presents a meticulously arranged display of Japanese [sweets](#) and a bottle of [sake](#) on two red lacquerware plates, set against a warm wooden table.



Captioner: ShareGPT

The dog's ears, a soft shape of pink, are [slightly perked up](#), adding a sense of alertness to its expression.



Text2Image: Stable-Diffusion

The train, located to [the bottom right of the image](#), emits rhythmic puffs as it travels through the dense, lush green forest, filled with tall pines that accentuate its presence.

Figure 3. **Examples of hallucinated sentences in AlignBench.** The hallucinated portions are often subtle, requiring fine-grained image-text alignment ability to detect them.

Hallucination detection and mitigation in image captioning. Hallucination detection in image captioning has been widely studied [43]. CHAIR [43] was the first metric to evaluate image-caption alignment at the object level using an object detector. However, its effectiveness is limited due to the detector’s coverage and accuracy. Besides, many works attempt to mitigate the hallucinations in image captions [15, 16, 25, 45, 56, 63, 65, 66], especially, mitigating hallucinations in long captions is important as they are prone to contain more hallucinations [21, 65], which we confirm in Sec. 3.3. Refining a captioning model based on image-caption alignment score computed by VLMs is a promising approach [13], and our work also contributes to this line of work. Despite these methodological developments and the use of VLMs as a detector, VLMs’ fundamental image-text alignment ability remains unclear. In our experiments, we focus on benchmarking diverse VLMs and clarifying their ability to align images and text.

3. Datasets

We aim to collect datasets that cover diverse image-caption pairs equipped with high-quality annotations of semantic alignment. This section first explains how we collect image-caption pairs and provide annotations to them, followed by an analysis of the dataset. We focus on obtaining labels for sentence-level semantic alignment for two reasons: (i) sentence-level labels give a cue to easily find more fine-detailed locations of unaligned descriptions, and (ii) span-level annotation suffers more from the subjectivity of annotation than sentence-level. For deeper analysis, we additionally provide span-level hallucination presence labels and categorize the types of hallucinations. Due to the limited space, we leave most details in the appendix.

3.1. Collecting Image-Caption Pairs

We aim to assess the ability to judge whether a given text-image pair is semantically aligned. Thus, coverage of diverse image domains and caption patterns is essential to building a benchmark. We thus obtain image-caption pairs using six image2text and two text2image models, where each *caption* consists of multiple consecutive sentences.

Image-to-text models (captioner). We employ CC12M [6] and the validation split of COCO 2017 [30] as image inputs. To ensure the diversity of the test images, we cluster images into 50 clusters and pick 40 images from each cluster, resulting in 2000 images in total. We manually categorize each cluster to enable interpretable analysis. We employ GPT-4o, ShareGPT (S-GPT) [8], LLaVA-NeXT [27], Llama-4 [35], Qwen 2 [53], and CogVLM [54], covering diverse architectures, scales, and openness. This diversity enables the collection of captions with differing levels of detail and language style. For each captioner-image pair, we apply a chat template (*e.g.*, “Describe the image in detail.”), yielding 12K outputs in total.

Text-to-image models. To ensure the diversity in a text prompt, we first pick 170 common object categories and prompt GPT-4o-mini [37] to include at least one of the categories and generate 3-4 sentences per prompt, resulting in 1000 prompts. To convert the prompts into images, we utilize Stable Diffusion 3.5 (SD) [44] as an open-source model and image generation model accessible through GPT-4o-mini (GPT-Gen), yielding 2K outputs in total.

3.2. Annotation

In the main paper, we focus on how to obtain labels for sentence-level semantic alignment and leave the fine-detailed annotation process in the appendix. We ask annotators to determine if the image presents all the details described in the text correctly. The use of SOTA models as captioners makes the annotation non-trivial because hallucinations produced by such models are often subtle and not immediately apparent at first glance, as shown in Fig. 3.

Annotation labels. We are inspired by the labeling scheme of [20], where annotators assign one of three categories: *correct*, *incorrect*, or *unknown*. An example of an annotation screen is illustrated on the right of Fig. 2. A sentence is labeled *correct* if it accurately describes the image, and *incorrect* if it contains a part that does not correctly describe the image. When correctness cannot be determined—for example, if the object is too small to recognize or if the description involves non-visible attributes such as smell or wind—it is labeled *unknown*. The *unknown* category is in-

Table 1. **Stats of AlignBench in sentence-level correctness annotations.** AlignBench contains a large number of annotated sentences, enough for benchmarking models. We exclude sentences with *unknown* label.

	Image-to-Caption (Captioners)						Text-to-Image		
	CogVLM	GPT4o	ShareGPT (S-GPT)	Llama-4	LLaVA-NeXT	Qwen-2	Stable Diffusion (SD)	gpt-image-1 (GPT-Gen)	Total
Sentences	7372	12790	17610	14800	15170	15790	2417	3524	89473
Sentences / Image	3.7	6.4	8.8	7.4	6.9	7.9	2.4	3.5	6.3
Positive / Total (%)	91.5	91.8	73.4	85.2	80.9	88.8	34.1	79.7	82.7
Word / Sentence	15.9	14.7	18.3	19.4	17.4	17.3	22.9	22.5	17.7

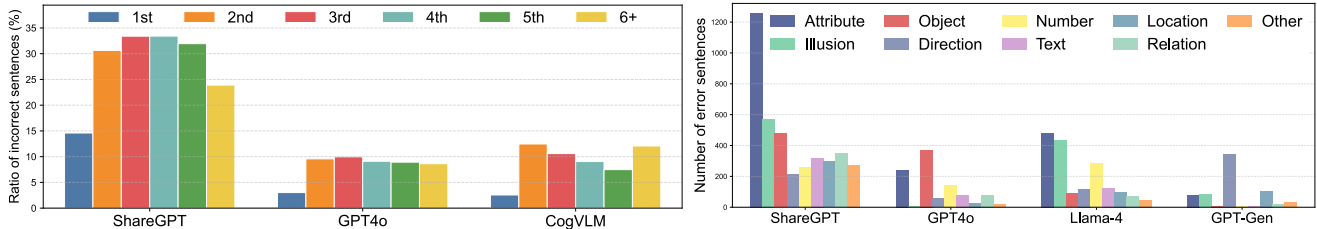


Figure 4. **Left:** Ratio of incorrect sentences by position; all captioners make fewer errors at the first position. Different colors indicate different positions. **Right:** Number of unaligned sentences per category; most mistakes occur in attributes and text.

Table 2. **Comparison with existing image-text alignment datasets.** AlignBench enables evaluation on longer sentences and a broader vocabulary, using outputs of diverse VLMs.

Dataset	# Sentences	Words/Sent.	Vocab	Sent. Generation
Foil [41]	5k	11.8	4.1k	Rule-base
HAT [41]	0.4k	13.6	1.2k	Rule-base
ARO [61]	2k	7.1	0.6k	Rule-base
Winoground [48]	1.6k	9.0	0.9k	Human
SugarCrepe [22]	2k	11.1	2.2k	Language Model
SeeTrue [58]	6.9k	11.5	1.5k	T2I model
GenAI-Bench [31]	1.6k	12.6	4.3k	T2I model
MHalDetect [20]	14k	18.0	4.4k	Captioner
AlignBench	89k	17.7	42k	Captioner + T2I

troduced to exclude unreliable cases from evaluation.

Annotation process. To ensure high-quality annotations, we adopt a two-stage process for sentence-level annotation: (i) crowd-sourced workers annotate each sentence, and (ii) we review the merged outcomes to guarantee quality. In the first stage, five independent workers annotate each sentence, reducing the risk of missing hallucinations. Moreover, their performance is continuously monitored through regular checks. The results are then merged based on majority voting, as detailed in the appendix, and subsequently reviewed. During the review, to minimize the inclusion of ambiguous cases in the evaluation, sentences that are difficult to judge are labeled as *unknown*. This process creates the dataset with sentence-level correctness annotations. We additionally provide annotator agreement scores as an indicator of task difficulty. We further annotate this dataset to provide segment-level hallucination presence labels and hallucination category labels, where hallucinations are categorized into eight types: *Attribute*, *Object*, *Number*, *Location*, *Illusion*, *Direction*, *Text*, *Relation*, and *Other*. These categories should reveal the weakness of the current VLMs

in understanding the image content.

3.3. Analysis of the Dataset

Examples of annotated sentences. Figure 3 presents unaligned image-sentence pairs. Captioners’ errors often involve visual details or object relationships rather than clear mistakes, making them hard to detect. Therefore, detectors need a fine-grained understanding of image-text alignment.

Basic stats. Table 1 summarizes the statistics of about 90K annotated *correct* or *incorrect* sentences. AlignBench provides correct and incorrect sentences enough for evaluation (excluding *unknown* cases). GPT-4o achieves the highest accuracy (91.8%) while Qwen (88.8%) and CogVLM (91.5%) perform comparably to GPT-4o among open-source VLMs. This suggests that a large number of outputs are needed to obtain sufficient incorrect samples for advanced captioners.

Comparison to existing image-text alignment datasets. Table 2 compares with existing image-text alignment datasets. AlignBench substantially surpasses prior datasets in scale, with over 89K sentences—one to two orders of magnitude larger than existing alignment benchmarks. It contains longer, image-caption pairs generated by captioner and T2I models, with a far richer vocabulary, enabling evaluation on diverse and long-tail concepts.

Positions of the hallucinations. The left of Fig. 4 computes the ratio of incorrect sentences in each position of the sentence. Across models, incorrect sentences appear most frequently in the second to fourth positions. This observation is consistent with previous work [21, 65]. The first sentence is less likely to contain hallucinations, likely because it often provides an overall image summary and language tokens attend to image features well.

Table 3. AUROC results across VLMs. Cells with the best performance within open-source and closed-source groups are highlighted in a blue background, while the best model within each model family is marked in bold.

Detector	Reference	Params	Image-to-Caption Models						Text-to-Image Models		Avg.
			S-GPT	Llava	Qwen-2	GPT4o	CogVLM	Llama-4 (109B)	SD	GPT-Gen	
Open-Source Models											
TripletCLIP	[40]	0.3B	50.7	51.9	53.9	53.9	51.0	50.9	48.2	44.9	50.7
SigLIP	[62]	0.2B	51.7	52.0	53.3	52.8	53.1	54.9	50.7	55.2	52.9
BLIP-2	[29]	1.2B	53.4	55.9	52.4	52.5	52.1	52.2	48.8	42.1	51.1
Phi-4	[1]	5.6B	54.2	53.1	52.5	51.4	51.9	50.8	52.6	50.9	52.1
Qwen-2	[53]	7B	60.2	55.3	55.9	46.0	51.9	53.2	54.6	46.0	52.9
Deepseek-VL2	[57]	27B	58.0	56.6	56.9	54.4	54.2	53.9	56.1	50.5	55.1
LLaVA-NeXT	[27]	72B	59.4	56.6	58.9	56.7	57.5	54.9	59.0	53.3	57.0
Pixtral-12B	[2]	12B	64.3	60.8	60.6	57.1	57.3	55.7	64.7	56.7	59.6
Gemma-3	[47]	12B	67.0	63.3	63.1	57.6	59.4	54.0	64.1	52.2	59.9
		27B	67.6	64.4	67.9	61.1	66.4	60.6	63.7	50.5	62.8
		2B	55.7	56.0	58.4	55.7	60.3	56.1	52.0	48.5	55.3
InternVL2	[12]	8B	66.6	65.7	69.1	63.9	67.6	60.6	64.3	52.5	63.8
		26B	63.9	60.6	61.2	57.1	58.9	55.6	53.1	43.8	56.8
		40B	69.3	63.0	66.5	59.6	61.9	61.5	69.5	56.5	63.4
InternVL2.5	[11]	78B	74.1	70.3	73.7	63.9	68.1	63.1	72.0	55.7	67.6
Qwen-2.5	[3]	7B	68.6	65.3	66.5	55.7	64.6	61.0	65.4	55.7	62.9
		32B	73.6	71.6	70.6	66.1	69.0	66.0	68.9	61.0	68.4
Llama-4	[35]	109B	80.7	78.6	77.6	67.5	77.2	<u>59.9</u>	81.1	64.7	73.4
		400B	81.1	80.9	79.0	71.9	81.3	64.7	83.0	67.8	76.2
Closed Models											
Gemini-2.0 Flash	[46]	N/A	76.8	73.5	74.9	65.5	70.4	64.8	73.4	57.0	69.5
GPT4o-mini		N/A	69.9	65.7	68.2	60.0	62.3	60.3	56.5	47.7	61.1
GPT4o		N/A	75.8	72.6	72.8	<u>58.2</u>	69.7	63.8	63.2	52.4	66.1
GPT4.1-mini	[37]	N/A	77.8	75.8	74.4	65.8	69.2	66.0	68.7	56.1	69.2
GPT5-mini		N/A	81.5	82.2	80.2	69.7	81.1	73.0	83.8	65.7	77.2
GPT5		N/A	85.4	86.0	85.3	72.3	85.5	78.4	84.9	72.0	81.2

Hallucination categories. We show the stats of hallucination types on the right of Fig. 4. Errors in *attributes* are the leading category for many models, indicating that adjectival descriptions (*e.g.*, color, texture) are prone to hallucination as indicated by Fig. 1 and 3. Also, many models tend to cause errors in *text*, probably because small texts are hard to read even with advanced models.

Difference between Image-to-Text and Text-to-Image models. We observe that T2I models, such as GPT-Gen, frequently make errors related to *Direction*, *e.g.*, the orientation of an eye or an object. This is likely because our text prompts often contain directional descriptions, which T2I models struggle to accurately represent.

4. Experiments

We aim to benchmark and analyze diverse VLMs on AlignBench to uncover key factors for building a performant image-text alignment model. After describing the experimental setup, we first present an overview of the empirical results, followed by a detailed analysis. In summary, our analysis reveals five key findings: (i) AlignBench spans diverse difficulty levels, enabling systematic

and interpretable evaluation; (ii) AlignBench serves as a new indicator of image–text alignment—models strong on AlignBench also perform well on prior benchmarks, while the reverse does not necessarily hold; (iii) CLIP-like models struggle to align pairs generated by modern captioners and T2I models; (iv) VLMs over-score early sentences regardless of correctness; and (v) evaluators show strong self-preference, consistently favoring their own outputs.

Setups. We aim to benchmark diverse VLMs in sentence-level image-text alignment, *i.e.*, the image presents all the details described in the single sentence correctly. Specifically, each sentence and image is independently fed into VLMs. We choose this evaluation protocol since the prior work on hallucination detection [36] and image-text alignment [22, 48, 58] also employs sentence-level evaluation. Following [5], we prompt the decoder-based VLMs to output the score of the alignment between the image and an input sentence, ranging from 0 to 100, as shown in the appendix. We also include BLIP-2 [29], TripletCLIP [40], and SigLIP [62] as fundamental image-text alignment models. Given the alignment score, we compute the AUROC within each captioner, which enables threshold-free evaluation,

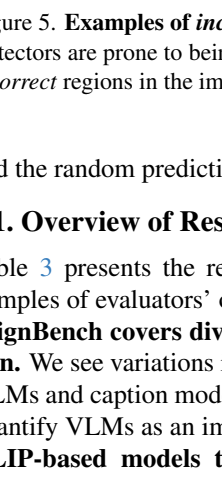
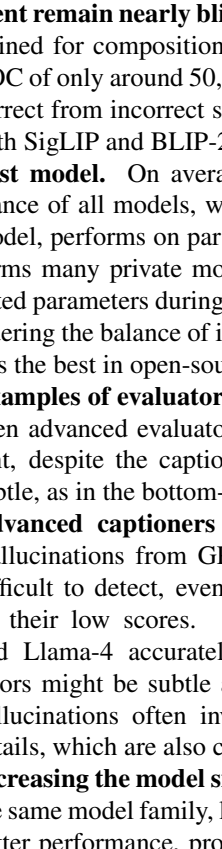
	<p>Captioner: LLaVA-Next</p> <p>The image shows a red and white fishing boat with the name "EMULATORE WY10" prominently displayed on its side.</p> <p>X Text</p> <table border="1"> <tr> <th></th><th>Llama-4</th><th>Gemma-27B</th><th>GPT5o-mini</th><th>Gemini</th></tr> <tr> <td></td><td>98</td><td>95</td><td>95</td><td>90</td></tr> </table>		Llama-4	Gemma-27B	GPT5o-mini	Gemini		98	95	95	90
	Llama-4	Gemma-27B	GPT5o-mini	Gemini							
	98	95	95	90							
	<p>Captioner: ShareGPT</p> <p>In the center of the image, a child stands in front of a table laden with a variety of food items.</p> <p>X Location</p> <table border="1"> <tr> <th></th> <th>Llama-4</th> <th>Gemma-27B</th> <th>GPT5o-mini</th> <th>Gemini</th> </tr> <tr> <td></td> <td>70</td> <td>90</td> <td>60</td> <td>100</td> </tr> </table>		Llama-4	Gemma-27B	GPT5o-mini	Gemini		70	90	60	100
	Llama-4	Gemma-27B	GPT5o-mini	Gemini							
	70	90	60	100							
	<p>Captioner: GPT-4o</p> <p>There is a person standing on the ground to the right, observing or interacting with the group.</p> <p>X Attribute</p> <table border="1"> <tr> <th></th> <th>Llama-4</th> <th>Gemma-27B</th> <th>GPT5o-mini</th> <th>Gemini</th> </tr> <tr> <td></td> <td>100</td> <td>90</td> <td>100</td> <td>100</td> </tr> </table>		Llama-4	Gemma-27B	GPT5o-mini	Gemini		100	90	100	100
	Llama-4	Gemma-27B	GPT5o-mini	Gemini							
	100	90	100	100							
	<p>Captioner: Text2Image: GPT-Gen</p> <p>In a vibrant jungle, a majestic tiger stands proudly on a rocky outcrop to the left, its powerful gaze fixed upon a flowing river below.</p> <p>X Direction</p> <table border="1"> <tr> <th></th> <th>Llama-4</th> <th>Gemma-27B</th> <th>GPT5o-mini</th> <th>Gemini</th> </tr> <tr> <td></td> <td>90</td> <td>95</td> <td>100</td> <td>100</td> </tr> </table>		Llama-4	Gemma-27B	GPT5o-mini	Gemini		90	95	100	100
	Llama-4	Gemma-27B	GPT5o-mini	Gemini							
	90	95	100	100							

Figure 5. Examples of *incorrect* sentences with detectors' correctness scores. Higher scores indicate greater confidence in correctness. Detectors are prone to being overconfident in these examples. We highlight detectors' errors in red within the text and mark the grounded *incorrect* regions in the image with orange boxes.

and the random prediction results in a score of 50.

4.1. Overview of Results

Table 3 presents the results evaluated on diverse VLMs. Samples of evaluators' outputs are available in Fig. 5.

AlignBench covers diverse levels of hallucination detection. We see variations in the performance across the tested VLMs and caption models. Thus, AlignBench is suitable to quantify VLMs as an image-text alignment model.

CLIP-based models tailored for compositional alignment remain nearly blind. TripletCLIP [40], despite being trained for compositional understanding, achieves an AUROC of only around 50, indicating that it fails to distinguish correct from incorrect sentences. The same trend holds for both SigLIP and BLIP-2.

Best model. On average, GPT-5 shows the best performance of all models, while Llama-4, the best open-source model, performs on par with GPT-5-mini. Llama-4 outperforms many private models with a large margin. Its activated parameters during inference are only 17B. When considering the balance of inference time and accuracy, Llama-4 is the best in open-source models.

Examples of evaluators' outputs. Figure 5 illustrates that even advanced evaluators can misinterpret the visual content, despite the captioners' errors not being particularly subtle, as in the bottom-left example.

Advanced captioners produces hard-to-detect errors. Hallucinations from GPT-4o, GPT-Gen, and Llama-4 are difficult to detect, even for proprietary models, as shown by their low scores. Since SOTA models like GPT-4o and Llama-4 accurately understand many scenes, their errors might be subtle and harder to identify. GPT-Gen's hallucinations often involve eye direction or fine visual details, which are also challenging.

Increasing the model size improves performance. Within the same model family, larger language models tend to yield better performance, probably because the task requires interpreting diverse captions.

Robustness to text-to-image models differs by VLMs.

Models such as Llama-4 and GPT-5-mini show the highest performance in SD across captioners, indicating that SD is the easiest split for these models. By contrast, for Gemma-3 (27B) and Qwen-2.5 (32B), the performance on SD is lower than S-GPT and Qwen-2. The difference should be due to the domains of images and the difference in language patterns. Inclusion of diverse data helps to find such trends.

4.2. Detailed Analysis

Hallucinations generated by better captioners are harder to detect. The left of Fig. 6 plots captioner performance on MMMU (x-axis) against AUROC measured by GPT-5-mini (y-axis). Captioners with higher MMMU scores tend to yield lower AUROC, indicating that stronger captioners generate hallucinations that are harder to detect.

The performance on AlignBench is highly correlated with that on MMMU. The right of Fig. 6 plots the performance on MMMU (x-axis) and AlignBench (y-axis), and indicates that models effective on MMMU perform well on AlignBench and vice versa.

Evaluators favor the sentence near the beginning of the caption. Figure 7 computes the detectors' output scores averaged within each sentence position. For both *correct* and *incorrect* image-text pairs, the detectors give a higher score to the sentences located near the beginning of the caption. The first sentence often provides the overview of the image, and VLMs seem to prefer such sentences irrespective of their correctness, possibly because such sentences are abundant in training datasets.

AlignBench serves as a new indicator of an image-text alignment capability. Table 4 compares AlignBench with existing hallucination-detection and VL-compositionality datasets. Although Gemma-3 slightly outperforms Llama-4 on Winoground, FOIL, and HAT, it underperforms by a large margin on many of the AlignBench tasks. This suggests that strong performance on short and simple sentences does not translate to the longer and more diverse

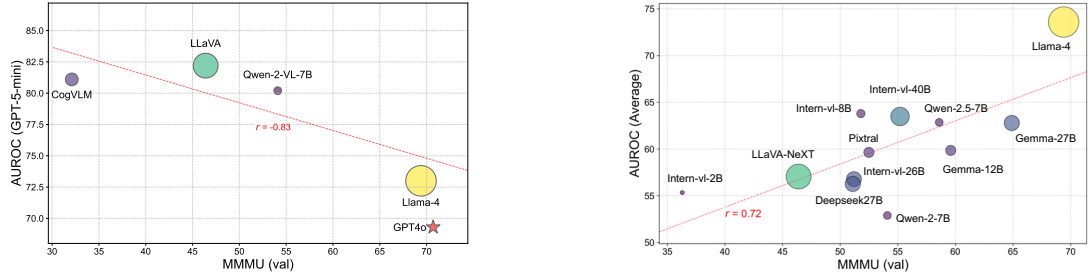


Figure 6. The size of plots indicates the parameter size. **Left:** MMMU performance measured on *Captioners* (X-axis) vs. AUROC measured by GPT-5-mini (Y-axis) for each Captioner. Advanced Captioners tend to produce errors that are difficult to detect. **Right:** MMMU (X-axis) vs. AUROC (Y-axis) for each *detector*. Detectors with better MMMU performance tend to perform better on AlignBench.

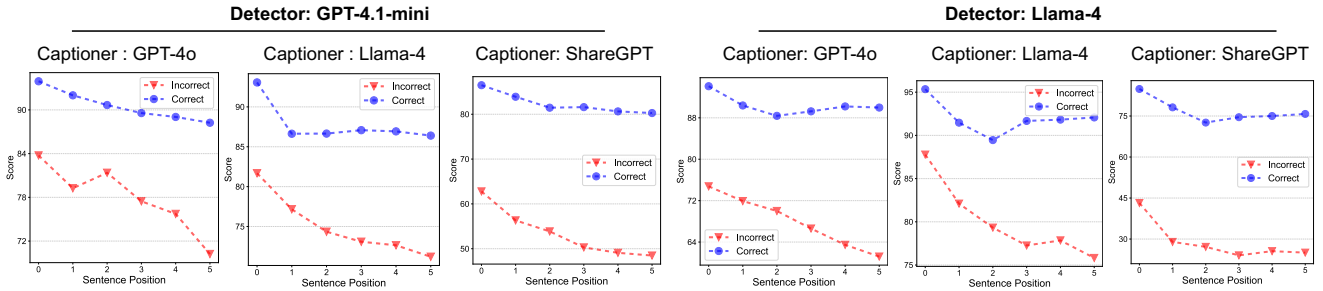


Figure 7. **Detectors show positional bias in scoring.** We average the detectors’ correctness scores (Y-axis) by sentence position (X-axis) and visualize the results using GPT-4o (Left) and Llama-4 (Right) as detectors. Both detectors assign higher scores to sentences appearing near the beginning of the output. The detector is *not* provided with any positional information during inference.

Table 4. **Comparison to existing datasets for hallucination detection and compositionality understanding (AUROC).** Results of prior benchmarks that exceed AlignBench are highlighted. Excelling on AlignBench indicates strong results on prior benchmarks.

Detector	Params	AlignBench					Hallucination Detection			VL-Compositionality			
		ShareGPT	Llava	GPT4o	Llama-4	CogVLM	MHalDetect	Foil	HAT	ARO	SugarCrepe	Winoground	SeeTrue
Qwen-2.5	7B	68.6	65.3	55.7	61.0	64.6	78.7	85.5	68.0	78.3	84.9	63.3	74.6
Qwen-2.5	32B	73.6	71.6	66.1	66.0	69.0	83.0	89.6	77.6	78.3	84.9	73.1	81.5
Gemma-3	27B	67.6	64.4	61.1	60.6	66.4	81.7	91.8	76.6	79.2	87.6	77.6	81.5
Llama-4	109B	80.8	78.7	67.8	59.9	77.2	82.8	90.3	76.3	84.8	89.4	77.1	83.1
GPT-5-mini	-	81.5	82.2	69.7	73.0	81.1	85.4	94.6	84.6	92.4	92.4	90.8	87.2

sentences in AlignBench. Conversely, Llama-4, which performs well on AlignBench, consistently shows strong results on these prior benchmarks, indicating that AlignBench better captures the broader alignment capabilities required across datasets. While detectors perform well on FOIL—indicating these hallucinations are easy for current SOTA VLMs—they perform poorly on Winoground and HAT, showing that even top models struggle with complex object compositions.

Detectors struggle to detect their own hallucinations. Table 3 shows that Llama-4 (109B) and GPT-4o perform poorly on their own outputs (highlighted by underline). This finding aligns with prior work reporting LLM evaluators favor their own outputs [39]. We annotate captions generated by Qwen-2.5 (32B) and Gemma-3 (27B) to enable more extensive self- and cross-evaluations. Figure 8

(left) confirms much lower AUROC on self-generated captions (diagonal elements). Figure 8 (right) shows that GPT-4o scores its own *incorrect* sentences higher than those of Llama-4, and the gap between incorrect and correct scores is small in its own output, which is causing the performance degradation.

Detectors are poor at detecting *Direction* and *Number* hallucinations. Figure 9 assesses detectors’ robustness across hallucination categories using their output scores (lower is better since only hallucinated sentences are accounted). *Direction* errors occur when object orientation is misdescribed; identifying the errors requires fine-grained visual understanding, and detectors consistently perform poorly. *Number* errors arise from incorrect object counts—an issue long recognized in early VLMs like CLIP [38] and still evident in advanced models.

Table 5. **Hallucinated segment localization results.** Each cell shows AP / mIoU (%). Localizing hallucinated segments remains difficult even for performant models.

Detector	Params	Image-to-Caption Models						Text-to-Image Models		Avg.
		S-GPT	Llava	Qwen-2	GPT4o	CogVLM	Llama-4	SD	GPT-Gen	
Qwen-2.5	32B	17.3 / 13.8	22.4 / 15.1	14.0 / 11.7	20.8 / 15.1	22.5 / 16.0	12.6 / 10.7	15.9 / 11.4	12.1 / 9.4	17.2 / 12.9
GPT-4o mini	-	25.2 / 21.6	28.9 / 22.4	20.6 / 18.3	29.5 / 23.3	28.0 / 21.5	18.7 / 16.4	14.7 / 12.5	14.6 / 11.9	22.5 / 18.5
Llama-4	109B	24.9 / 22.6	27.0 / 20.8	24.8 / 22.7	34.3 / 26.4	29.3 / 23.2	19.6 / 17.3	15.1 / 10.7	11.0 / 9.0	23.3 / 19.1
Llama-4	400B	28.2 / 24.8	29.1 / 22.1	26.2 / 23.3	34.0 / 26.0	29.8 / 21.7	19.4 / 18.0	15.4 / 11.9	12.0 / 9.3	24.2 / 19.6

Table 6. **Ensembling detectors’ outputs improves performance in almost all cases.** The increase or decrease from the *better* model used for ensembling is highlighted next to each score.

Detector 1	Detector 2	Image-to-Caption Models						Text-to-Image Models	
		S-GPT	Llava	Qwen-2	GPT4o	CogVLM	Llama-4	SD	GPT-Gen
Qwen-2.5 (7B)	Gemma-3 (27B)	71.9 (+3.3)	68.4 (+4.0)	71.3 (+3.4)	64.6 (+3.5)	69.3 (+2.9)	63.3 (+2.3)	67.6 (+2.2)	54.8 (-0.9)
Llama-4 (109B)	LLlama-4 (400B)	84.6 (+3.5)	83.4 (+2.4)	82.9 (+3.9)	74.0 (+2.1)	83.5 (+2.2)	65.8 (+1.1)	84.6 (+1.6)	69.1 (+1.2)
Llama-4 (109B)	GPT5-mini	86.0 (+4.5)	84.8 (+2.7)	83.6 (+3.4)	73.9 (+4.2)	84.4 (+3.2)	72.3 (-0.7)	85.2 (+1.4)	68.6 (+2.9)

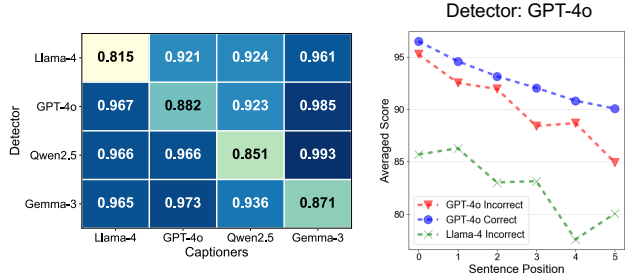


Figure 8. **Detectors struggle to detect their own hallucination.** **Left:** Self- and cross-evaluation results. AUROC scores for each Captioner (columns), normalized by the average AUROC of each Detector (rows). Diagonal entries show self-evaluation. **Right:** We pick GPT-4o as a detector, with their output correctness scores averaged by sentence position. **Blue** and **red** lines show scores for *correct* and *incorrect* GPT-4o’s outputs; **green** shows scores for *incorrect* Llama-4 outputs.

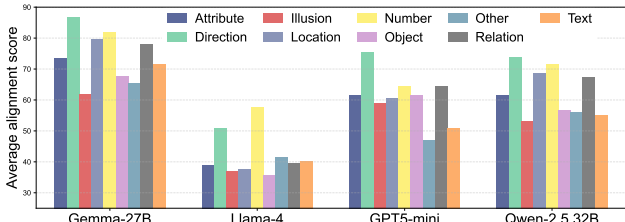


Figure 9. **Detectors’ score averaged within each hallucination type.** Detectors show weakness in *Direction* and *Number*.

Segment-level localization has more room for improvement. AlignBench includes hallucination segments for each hallucinated sentence, enabling segment-level evaluation. We present VLMs with a hallucinated sentence-image pair and prompt them to localize the hallucinated

span, explicitly noting that one exists. Performance is measured by alignment with human annotations (see Appendix for prompts and metrics). As shown in Table 5, Llama-4 (400B), the best model, localizes only 24.2% of hallucinated segments on average, underscoring substantial room for improvement. Notably, GPT-4o mini outperforms Qwen-2.5 (32B), in contrast to Table 3, indicating that strong sentence-level detectors are not always effective for segment-level localization.

Ensembling improves performance. We study whether ensembling improves detection. We average alignment scores from two comparably strong models (Table 3) and observe consistent gains (Table 6). This suggests that models apply distinct criteria for image-caption alignment, and combining them enhances performance. A drop occurs for ensembling Llama-4 and GPT-5-mini on Llama-4 captions, likely due to the large performance gap between the two models.

Contents in the appendix. Refer to the appendix for more empirical results. We give their overview below.

1. We provide a comparison with the prior approach in hallucination detection in image captioning, indicating that VLM-based detectors can surpass the prior one with a large margin.
2. The chain-of-thought and self-ensembling are effective in improving the performance of detectors.
3. More visualizations of annotation and detectors’ outputs.
4. Detailed stats of AlignBench.

5. Conclusion

We introduced AlignBench, a benchmark for evaluating hallucination detection in image captioning across diverse models, domains, and fine-grained annotations. Our analysis shows that CLIP-like models are nearly blind to hallu-

cinations, VLMs over-score early sentences, and detectors exhibit strong self-preference. Importantly, performance on AlignBench reliably predicts performance on existing benchmarks, while the reverse does not necessarily hold, positioning AlignBench as a new and more comprehensive indicator of image–text alignment. We expect it to support the development of a better alignment model.

Acknowledgement. This work is supported by JST Moonshot R&D Program Grant Number JPMJMS2236. This work is supported by “TSUBAME Encouragement Program for Young/Female Users” of Center for Information Infrastructure at Institute of Science Tokyo and by “Joint Usage/Research Center for Interdisciplinary Large-scale Information Infrastructures” in Japan.

References

- [1] Abdelrahman Abouelenin, Atabak Ashfaq, Adam Atkinson, Hany Awadalla, Nguyen Bach, Jianmin Bao, Alon Ben-haim, Martin Cai, Vishrav Chaudhary, Congcong Chen, et al. Phi-4-mini technical report: Compact yet powerful multimodal language models via mixture-of-loras. *arXiv preprint arXiv:2503.01743*, 2025. 5
- [2] Pravesh Agrawal, Szymon Antoniak, Emma Bou Hanna, Baptiste Bout, Devendra Chaplot, Jessica Chudnovsky, Diogo Costa, Baudouin De Moncault, Saurabh Garg, Theophile Gervet, et al. Pixtral 12b. *arXiv preprint arXiv:2410.07073*, 2024. 5
- [3] Shuai Bai, Keqin Chen, Xuejing Liu, Jialin Wang, Wenbin Ge, Sibo Song, Kai Dang, Peng Wang, Shijie Wang, Jun Tang, et al. Owen2. 5-vl technical report. *arXiv preprint arXiv:2502.13923*, 2025. 5
- [4] Manuele Barraco, Marcella Cornia, Silvia Cascianelli, Lorenzo Baraldi, and Rita Cucchiara. The unreasonable effectiveness of clip features for image captioning: an experimental analysis. In *CVPR*, 2022. 1
- [5] David Chan, Suzanne Petryk, Joseph E Gonzalez, Trevor Darrell, and John Canny. Clair: Evaluating image captions with large language models. In *EMNLP*, 2023. 5
- [6] Soravit Changpinyo, Piyush Sharma, Nan Ding, and Radu Soricut. Conceptual 12m: Pushing web-scale image-text pre-training to recognize long-tail visual concepts. In *CVPR*, 2021. 3
- [7] Jun Chen, Deyao Zhu, Xiaoqian Shen, Xiang Li, Zechun Liu, Pengchuan Zhang, Raghuraman Krishnamoorthi, Vikas Chandra, Yunyang Xiong, and Mohamed Elhoseiny. Minigpt-v2: large language model as a unified interface for vision-language multi-task learning. *arXiv preprint arXiv:2310.09478*, 2023. 1
- [8] Lin Chen, Jinsong Li, Xiaoyi Dong, Pan Zhang, Conghui He, Jiaqi Wang, Feng Zhao, and Dahu Lin. Sharegpt4v: Improving large multi-modal models with better captions. In *ECCV*, pages 370–387. Springer, 2024. 3
- [9] Runnan Chen, Youquan Liu, Lingdong Kong, Xinge Zhu, Yuexin Ma, Yikang Li, Yuenan Hou, Yu Qiao, and Wenping Wang. Clip2scene: Towards label-efficient 3d scene understanding by clip. In *CVPR*, pages 7020–7030, 2023. 1
- [10] Xiang Chen, Chenxi Wang, Yida Xue, Ningyu Zhang, Xiaoyan Yang, Qiang Li, Yue Shen, Lei Liang, Jinjie Gu, and Huajun Chen. Unified hallucination detection for multi-modal large language models. In *ACL*, 2024. 2, 16, 19, 20
- [11] Zhe Chen, Weiyun Wang, Yue Cao, Yangzhou Liu, Zhangwei Gao, Erfei Cui, Jinguo Zhu, Shenglong Ye, Hao Tian, Zhaoyang Liu, et al. Expanding performance boundaries of open-source multimodal models with model, data, and test-time scaling. *arXiv preprint arXiv:2412.05271*, 2024. 5
- [12] Zhe Chen, Weiyun Wang, Hao Tian, Shenglong Ye, Zhangwei Gao, Erfei Cui, Wenwen Tong, Kongzhi Hu, Jiapeng Luo, Zheng Ma, et al. How far are we to gpt-4v? closing the gap to commercial multimodal models with open-source suites. *arXiv preprint arXiv:2404.16821*, 2024. 5
- [13] Ailin Deng, Zhirui Chen, and Bryan Hooi. Seeing is believing: Mitigating hallucination in large vision-language models via clip-guided decoding. *arXiv preprint arXiv:2402.15300*, 2024. 3
- [14] António Farinhas, José GC de Souza, and André FT Martins. An empirical study of translation hypothesis ensembling with large language models. In *EMNLP*, 2023. 19
- [15] Sebastian Farquhar, Jannik Kossen, Lorenz Kuhn, and Yarin Gal. Detecting hallucinations in large language models using semantic entropy. *Nature*, 630(8017):625–630, 2024. 3
- [16] Alessandro Favero, Luca Zancato, Matthew Trager, Siddharth Choudhary, Pramuditha Perera, Alessandro Achille, Ashwin Swaminathan, and Stefano Soatto. Multi-modal hallucination control by visual information grounding. In *CVPR*, 2024. 3
- [17] Joseph Fleiss. Measuring nominal scale agreement among many raters. *Psychological Bulletin*, 76:378–382, 1971. 13
- [18] Chaoyou Fu, Peixian Chen, Yunhang Shen, Yulei Qin, Mengdan Zhang, Xu Lin, Jinrui Yang, Xiawu Zheng, Ke Li, Xing Sun, et al. Mme: A comprehensive evaluation benchmark for multimodal large language models. *arXiv preprint arXiv:2306.13394*, 2023. 2
- [19] Tianrui Guan, Fuxiao Liu, Xiyang Wu, Ruiqi Xian, Zongxia Li, Xiaoyu Liu, Xijun Wang, Lichang Chen, Furong Huang, Yaser Yacoob, et al. Hallusionbench: an advanced diagnostic suite for entangled language hallucination and visual illusion in large vision-language models. In *CVPR*, pages 14375–14385, 2024. 2
- [20] Anisha Gunjal, Jihan Yin, and Erhan Bas. Detecting and preventing hallucinations in large vision language models. In *AAAI*, 2024. 2, 3, 4, 16
- [21] Yusuke Hirota, Boyi Li, Ryo Hachiuma, Yueh-Hua Wu, Boris Ivanovic, Yuta Nakashima, Marco Pavone, Yejin Choi, Yu-Chiang Frank Wang, and Chao-Han Huck Yang. Lotus: A leaderboard for detailed image captioning from quality to societal bias and user preferences. In *ACL*, 2025. 3, 4
- [22] Cheng-Yu Hsieh, Jieyu Zhang, Zixian Ma, Aniruddha Kembhavi, and Ranjay Krishna. Sugarcrepe: Fixing hackable benchmarks for vision-language compositionality. *NeurIPS*, 2023. 1, 2, 4, 5, 16
- [23] Hugging Face. Hugging face. 12

[24] Dongfu Jiang, Xiang Ren, and Bill Yuchen Lin. Llm-blender: Ensembling large language models with pairwise ranking and generative fusion. In *ACL*, 2023. 19

[25] Sicong Leng, Hang Zhang, Guanzheng Chen, Xin Li, Shijian Lu, Chunyan Miao, and Lidong Bing. Mitigating object hallucinations in large vision-language models through visual contrastive decoding. In *CVPR*, 2024. 3

[26] Bohao Li, Yuying Ge, Yixiao Ge, Guangzhi Wang, Rui Wang, Ruimao Zhang, and Ying Shan. Seed-bench: Benchmarking multimodal large language models. In *CVPR*, pages 13299–13308, 2024. 2

[27] Bo Li, Kaichen Zhang, Hao Zhang, Dong Guo, Renrui Zhang, Feng Li, Yuanhan Zhang, Ziwei Liu, and Chunyuan Li. Llava-next: Stronger llms supercharge multimodal capabilities in the wild, 2024. 3, 5

[28] Junnan Li, Dongxu Li, Caiming Xiong, and Steven Hoi. Blip: Bootstrapping language-image pre-training for unified vision-language understanding and generation. In *ICML*. PMLR, 2022. 1

[29] Junnan Li, Dongxu Li, Silvio Savarese, and Steven Hoi. Blip-2: Bootstrapping language-image pre-training with frozen image encoders and large language models. In *ICML*. PMLR, 2023. 1, 5

[30] Tsung-Yi Lin, Michael Maire, Serge Belongie, James Hays, Pietro Perona, Deva Ramanan, Piotr Dollár, and C Lawrence Zitnick. Microsoft coco: Common objects in context. In *ECCV*, pages 740–755, 2014. 3

[31] Zhiqiu Lin, Deepak Pathak, Baiqi Li, Jiayao Li, Xide Xia, Graham Neubig, Pengchuan Zhang, and Deva Ramanan. Evaluating text-to-visual generation with image-to-text generation. In *ECCV*, 2024. 2, 4, 16

[32] Haotian Liu, Chunyuan Li, Qingyang Wu, and Yong Jae Lee. Visual instruction tuning. *NeurIPS*, 36:34892–34916, 2023. 1

[33] Haotian Liu, Chunyuan Li, Yuheng Li, and Yong Jae Lee. Improved baselines with visual instruction tuning. In *CVPR*, 2024. 1

[34] Pan Lu, Hritik Bansal, Tony Xia, Jiacheng Liu, Chunyuan Li, Hannaneh Hajishirzi, Hao Cheng, Kai-Wei Chang, Michel Galley, and Jianfeng Gao. Mathvista: Evaluating mathematical reasoning of foundation models in visual contexts. *arXiv preprint arXiv:2310.02255*, 2023. 2

[35] Meta.AI. The llama 4 herd: The beginning of a new era of natively multimodal ai innovation, 2025. 3, 5

[36] Abhika Mishra, Akari Asai, Vidhisha Balachandran, Yizhong Wang, Graham Neubig, Yulia Tsvetkov, and Hannaneh Hajishirzi. Fine-grained hallucination detection and editing for language models. In *COLM*, 2024. 5, 12

[37] OpenAI. ChatGPT. <https://chat.openai.com/chat>, 2023. 3, 5

[38] Roni Paiss, Ariel Ephrat, Omer Tov, Shiran Zada, Inbar Mosseri, Michal Irani, and Tali Dekel. Teaching clip to count to ten. In *ICCV*, pages 3170–3180, 2023. 7

[39] Arjun Panickssery, Samuel Bowman, and Shi Feng. Llm evaluators recognize and favor their own generations. *NeurIPS*, 2024. 2, 7

[40] Maitreya Patel, Naga Sai Abhiram Kusumba, Sheng Cheng, Changhoon Kim, Tejas Gokhale, Chitta Baral, et al. Triplet-clip: Improving compositional reasoning of clip via synthetic vision-language negatives. *NeurIPS*, 2024. 1, 5, 6

[41] Suzanne Petryk, David M Chan, Anish Kachinthaya, Haodi Zou, John Canny, Joseph E Gonzalez, and Trevor Darrell. Aloha: A new measure for hallucination in captioning models. In *ACL*, 2024. 4, 16

[42] Alec Radford, Jong Wook Kim, Chris Hallacy, Aditya Ramesh, Gabriel Goh, Sandhini Agarwal, Girish Sastry, Amanda Askell, Pamela Mishkin, Jack Clark, et al. Learning transferable visual models from natural language supervision. In *ICML*, 2021. 1

[43] Anna Rohrbach, Lisa Anne Hendricks, Kaylee Burns, Trevor Darrell, and Kate Saenko. Object hallucination in image captioning. In *EMNLP*, 2018. 3

[44] Stability AI. Stable diffusion 3.5 large. <https://stability.ai/news/introducing-stable-diffusion-3-5>, 2024. 3

[45] Wei Suo, Lijun Zhang, Mengyang Sun, Lin Yuanbo Wu, Peng Wang, and Yanning Zhang. Octopus: Alleviating hallucination via dynamic contrastive decoding. In *CVPR*, 2025. 3

[46] Gemini team. Gemini 2.0 flash, 2024. 5

[47] Gemma Team, Aishwarya Kamath, Johan Ferret, Shreya Pathak, Nino Vieillard, Ramona Merhej, Sarah Perrin, Tatiana Matejovicova, Alexandre Ramé, Morgane Rivière, et al. Gemma 3 technical report. *arXiv preprint arXiv:2503.19786*, 2025. 5

[48] Tristan Thrush, Ryan Jiang, Max Bartolo, Amanpreet Singh, Adina Williams, Douwe Kiela, and Candace Ross. Winoground: Probing vision and language models for visio-linguistic compositionality. In *Proceedings of the IEEE/CVF Conference on Computer Vision and Pattern Recognition*, pages 5238–5248, 2022. 1, 2, 4, 5, 16

[49] Peter Tong, Ellis Brown, Penghao Wu, Sanghyun Woo, Adithya Jairam Vedagiri IYER, Sai Charitha Akula, Shusheng Yang, Jihan Yang, Manoj Middepogu, Ziteng Wang, et al. Cambrian-1: A fully open, vision-centric exploration of multimodal llms. *NeurIPS*, 37:87310–87356, 2024. 2

[50] Shengbang Tong, Zhuang Liu, Yuexiang Zhai, Yi Ma, Yann LeCun, and Saining Xie. Eyes wide shut? exploring the visual shortcomings of multimodal llms. In *CVPR*, pages 9568–9578, 2024. 2

[51] Yuiga Wada, Kazuki Matsuda, Komei Sugiura, and Graham Neubig. Zina: Multimodal fine-grained hallucination detection and editing. *arXiv preprint arXiv:2506.13130*, 2025. 2, 16

[52] Junyang Wang, Yiyang Zhou, Guohai Xu, Pengcheng Shi, Chenlin Zhao, Haiyang Xu, Qinghao Ye, Ming Yan, Ji Zhang, Jihua Zhu, et al. Evaluation and analysis of hallucination in large vision-language models. *arXiv preprint arXiv:2308.15126*, 2023. 2, 16

[53] Peng Wang, Shuai Bai, Sinan Tan, Shijie Wang, Zhihao Fan, Jinze Bai, Keqin Chen, Xuejing Liu, Jialin Wang, Wenbin Ge, et al. Qwen2-vl: Enhancing vision-language model's

perception of the world at any resolution. *arXiv preprint arXiv:2409.12191*, 2024. 1, 3, 5

[54] Weihan Wang, Qingsong Lv, Wenmeng Yu, Wenyi Hong, Ji Qi, Yan Wang, Junhui Ji, Zhuoyi Yang, Lei Zhao, Song XiXuan, et al. Cogvlm: Visual expert for pretrained language models. *NeurIPS*, 2024. 3

[55] Jason Wei, Xuezhi Wang, Dale Schuurmans, Maarten Bosma, Fei Xia, Ed Chi, Quoc V Le, Denny Zhou, et al. Chain-of-thought prompting elicits reasoning in large language models. In *NeurIPS*, 2022. 19

[56] Sangmin Woo, Donguk Kim, Jaehyuk Jang, Yubin Choi, and Changick Kim. Don't miss the forest for the trees: Attentional vision calibration for large vision language models. In *ACL Findings*, 2025. 3

[57] Zhiyu Wu, Xiaokang Chen, Zizheng Pan, Xingchao Liu, Wen Liu, Damai Dai, Huazuo Gao, Yiyang Ma, Chengyue Wu, Bingxuan Wang, Zhenda Xie, Yu Wu, Kai Hu, Jiawei Wang, Yaofeng Sun, Yukun Li, Yishi Piao, Kang Guan, Aixin Liu, Xin Xie, Yuxiang You, Kai Dong, Xingkai Yu, Haowei Zhang, Liang Zhao, Yisong Wang, and Chong Ruan. Deepseek-vl2: Mixture-of-experts vision-language models for advanced multimodal understanding. *arXiv preprint arXiv:2412.10302*, 2024. 5

[58] Michal Yarom, Yonatan Bitton, Soravit Changpinyo, Roei Aharoni, Jonathan Herzig, Oran Lang, Eran Ofek, and Idan Szpektor. What you see is what you read? improving text-image alignment evaluation. *NeurIPS*, 2023. 2, 4, 5, 16

[59] Xiang Yue, Yuansheng Ni, Kai Zhang, Tianyu Zheng, Ruoqi Liu, Ge Zhang, Samuel Stevens, Dongfu Jiang, Weiming Ren, Yuxuan Sun, et al. Mmmu: A massive multi-discipline multimodal understanding and reasoning benchmark for expert agi. In *CVPR*, pages 9556–9567, 2024. 2

[60] Xiang Yue, Tianyu Zheng, Yuansheng Ni, Yubo Wang, Kai Zhang, Shengbang Tong, Yuxuan Sun, Botao Yu, Ge Zhang, Huan Sun, et al. Mmmu-pro: A more robust multi-discipline multimodal understanding benchmark. In *ACL*, 2025. 2

[61] Mert Yuksekgonul, Federico Bianchi, Pratyusha Kalluri, Dan Jurafsky, and James Zou. When and why vision-language models behave like bags-of-words, and what to do about it? In *ICLR*, 2023. 1, 2, 4, 16

[62] Xiaohua Zhai, Basil Mustafa, Alexander Kolesnikov, and Lucas Beyer. Sigmoid loss for language image pre-training. In *ICCV*, 2023. 5

[63] Ruiyang Zhang, Hu Zhang, and Zhedong Zheng. VI-uncertainty: Detecting hallucination in large vision-language model via uncertainty estimation. *arXiv preprint arXiv:2411.11919*, 2024. 3

[64] Kaiyang Zhou, Jingkang Yang, Chen Change Loy, and Ziwei Liu. Learning to prompt for vision-language models. *IJCV*, 130(9):2337–2348, 2022. 1

[65] Yiyang Zhou, Chenhang Cui, Jaehong Yoon, Linjun Zhang, Zhun Deng, Chelsea Finn, Mohit Bansal, and Huaxiu Yao. Analyzing and mitigating object hallucination in large vision-language models. In *ICLR*, 2024. 3, 4

[66] Xianwei Zhuang, Zhihong Zhu, Yuxin Xie, Liming Liang, and Yuexian Zou. Vasparse: Towards efficient visual hallucination mitigation via visual-aware token sparsification. In *CVPR*, 2025. 3

Supplementary Material for AlignBench

A. Limitation

Methodology. HalDec needs to be a light-weight model, considering its application to curate datasets. However, our results indicate that VLMs with more parameters show superior performance. Also, our evaluation relies on sentence-by-sentence score output, which regards each sentence as independent. However, this protocol ignores the context of consecutive sentences. We observe that many sentences can be regarded as independent, yet considering multiple sentences together might improve the performance of hallucination detection.

Annotations. Judging the hallucinations in image captions involves subjective criteria of annotators. Captions may look hallucinated to some annotators, while they do not to others. Having a unified consensus on this criterion is difficult. For sentence-level annotation, we introduce a category *unknown*, which allows us to exclude such ambiguous samples during evaluation. This issue can be more significant in segment localization and categorizing hallucination types. Then, we focus on sentence-level detection to benchmark VLMs following Mishra et al. [36].

B. The Use of Large Language Models (LLMs)

In preparing this manuscript, we made limited use of large language models (LLMs) such as ChatGPT. Specifically, LLMs were employed only to assist with polishing the writing for grammar, clarity, and readability. No part of the research design, analysis, interpretation, or results was generated or influenced by LLMs. All scientific content, data, and conclusions are the sole work of the authors.

C. Attribution to an icon

We employ the chatbot icons created by Freepik - Flaticon³ for Fig. 1.

D. Dataset

D.1. Image-Caption Collection

We describe the list of models used for collection in Table A. All models except for closed ones are downloaded from Hugging Face [23].

Table A. Details of VLMs picked as Captioners and Text2Image models. We cover diverse models considering their size, provider, and release date.

Model	Provider	Open/Closed	Scale	Release
GPT-4o	OpenAI	Closed	-	2024/05
ShareGPT (Share Captioner)	Shanghai AI Laboratory	Open	7B	2023/11
LLaVA-NeXT (llava-next-72b-hf)	Microsoft	Open	72B	2024/01
Llama-4-Scout (17B-16E)	Meta	Open	109B	2025/04
Qwen2.5-VL (7B-Instruct)	Alibaba	Open	7B	2024/12
CogVLM (coglm2-llama3-chat-19B)	Tsinghua Univ.	Open	19B	2024/06
Stable-diffusion-3.5-medium (SD)	Stability AI	Open	2.5B	2024/10
GPT-Gen (GPT4o-mini)	OpenAI	Closed	-	2024/05

Captioner models. We collect data from two sources and employ two text-to-image models. The first source is CC12M, which is designed for vision-and-language pre-training and provides broad domain coverage. The second source is the COCO 2017 dataset, where we use the validation split. For both datasets, we cluster images into 50 domains based on ResNet features and then sample 40 images from each cluster, resulting in a total of 2,000 images per dataset.

For the Captioner models, we randomly select one of the following instructions:

³<https://www.flaticon.com/free-icons/chatbot>

Instruction given to captioner models

1. Describe this image in detail.
2. Describe this image in detail. Instead of describing the imaginary content, only describe the content one can determine confidently from the image.
3. Provide a detailed description of the image, but only include elements that are clearly visible and verifiable.
4. Describe this image in detail. Minimize aesthetic descriptions as much as possible.
5. Provide a detailed, factual description without using emotional language.

Text-to-image models. We employ two text-to-image models. The first is stabilityai/stable-diffusion-3.5-medium, a diffusion-based generative model that we run locally via the Diffusers library on GPU hardware. The second is OpenAI’s gpt-image-1, which is accessed through the Responses API with gpt-4o-mini acting as the controller for image generation. For both models, we use identical prompts. To encourage category diversity, we predefine 170 object categories and randomly select one to be included in each prompt. The selected category is then inserted into an instruction given to gpt-4o-mini, which produces a 3–4 sentence description following the specification below.

Instruction given to GPT-4o-mini for producing text-to-image prompts

I want to create prompts to generate image using text to image model. The prompts need to satisfy the following criteria.

1. The prompts include 3-4 sentences.
2. They need to describe a scene including target.
3. They need to describe the state of the objects, what they are doing.
4. They need to describe the location of the object in image, (e.g., left, right, bottom, top, etc)
5. They also need to describe where the objects are looking at (e.g., left, right, bottom, top, or towards some) if the object is some organism.

Can you suggest a prompt? Please return in the form of dictionary, with a key of “prompt”.

Output:

D.2. Voting and Quality Control

We first recruited five annotators and conducted a pilot on one hundred images. The authors reviewed all annotations, and annotators who failed to meet our quality standards were not assigned further items. This process allowed us to identify trusted annotators. Each trusted annotator was then assigned between one thousand and two thousand images. The authors checked the quality for every batch of about two hundred images. If the annotations did not meet our standards, annotators were required to re-annotate before proceeding.

After the main annotation, we applied multi-round voting. Annotator-specific weights were assigned, with trusted annotators given higher weights. The aggregated votes were used to determine the final labels. For the *incorrect* (hallucination) category, we adopted a stricter rule: if one trusted annotator or two annotators labeled an item as incorrect, the authors manually reviewed it, since hallucinations are more difficult to detect reliably than correctness. Finally, the authors adjudicated all ambiguous cases. This combination of pilot screening, ongoing audits, weighted voting, and final review ensured high-quality hallucination detection annotations.

D.3. Inter-Annotator Agreement

We evaluated inter-annotator consistency on AlignBench using Fleiss’ kappa [17] with three labels (correct/incorrect/unknown). The overall agreement reached $\kappa = 0.28$ with an observed agreement of $P_{\text{bar}} = 0.77$, which is reasonable given the strong class imbalance in the dataset. When analyzing per-model subsets, the highest agreement was observed for cogvlm with $\kappa = 0.40$, indicating that its outputs tend to yield more consistent judgments. In contrast, the lowest agreement appeared for gpt4o, which achieved $\kappa = 0.22$ despite a high observed agreement ($P_{\text{bar}} = 0.86$), suggesting that its infrequent errors are more ambiguous and therefore harder to annotate. Importantly, the authors manually adjudicated all samples that received conflicting labels from annotators.

Caption Annotation Tool

15 / 2000

The image depicts a large stone statue of a human figure holding an object in front of an architectural structure.

The figure is robed and stands upright with eyes slightly closed and a neutral expression.

It holds a spherical object emitting a bright light.

Behind the statue are two tall, cone-shaped towers with flat tops and crosses.

The towers are part of a red-brick building with white accents and contain multiple arched windows.

The central part of the building features a circular clock above an entrance.

The sky above is partly cloudy.

Figure A. Example of an interface used for the hallucination detection.

D.4. Annotator Recruitment

For the hallucination detection task, we recruited crowd annotators and offered compensation based on the phase and level of effort. On average, annotators received around \$100 for completing 2,000 images during the detection phase. Since the hallucination type annotation required more careful reading and reasoning, the compensation was higher, averaging around \$150 for each model output. The exact amount varied slightly depending on the annotator's country of residence. We did not restrict annotators by location, but we required strong English reading skills, which were verified during the pilot stage. We recruited annotators on Upwork⁴, Freelancer⁵, and CrowdWorks⁶.

Figure A shows the annotation interface for the hallucination detection phase, while Figure B shows the interface used for the hallucination type annotation phase.

D.5. Hallucination Type and Location Annotation

Table B shows the eight hallucination type categories used in the HalCap dataset. These categories cover both fine-grained object- and attribute-level mistakes as well as broader contextual errors. Figure C shows annotation examples for each error

⁴<https://www.upwork.com/>

⁵<https://www.freelancer.com/>

⁶<https://crowdworks.jp/>

Error Annotation

Model: sd

Prev 21 Go Next

Image 21/867



In a sunlit garden, a vibrant orange carrot is nestled in rich, dark soil on the left side of the image, **partially** exposed as if it is peeking out from the ground.

Object Attribute Number Text Relation Location Direction Illusion Other Unknown More

To its right, a curious rabbit with soft, white fur is intently **looking at the carrot**, its ears perked up in excitement.

Object Attribute Number Text Relation Location Direction Illusion Other Unknown More

In the background, blooming flowers sway gently in the breeze, their colors contrasting beautifully with the earthy tones of the soil.

Object Attribute Number Text Relation Location Direction Illusion Other Unknown More

Above the scene, **a clear blue sky** adds to the serene atmosphere, casting gentle light over the garden.

Object Attribute Number Text Relation Location Direction Illusion Other Unknown More

Figure B. Example of an interface used for the hallucination type annotation.

Table B. Types of hallucinations categorized for analysis.

Type	Description
Object	Misidentifies an object or uses an incorrect noun (e.g., calling a dog a cat).
Attribute	Incorrect description of an object's property such as color, size, or action (e.g., red car described as blue).
Number	Incorrectly states the number of objects or people (e.g., "three people" when only two are present).
Text	Misreads or misrepresents textual information in the image (e.g., misreading a store sign).
Relation	Incorrect description of relationships between objects (e.g., "a man riding a horse" when he is standing next to it).
Location	Misrepresents the position of an object in the image (e.g., "a cup on the table" when it is on the floor).
Direction	Incorrectly describes the direction/orientation of an object (e.g., "a person facing left" when they face right).
Illusion	Describes objects, scenes, or actions that do not exist at all (e.g., mentioning "a flying bird" when no bird is present).

type. Hallucinations are highlighted in red.

D.6. Additional Analysis

Detailed comparison against existing datasets. Table C describes the detailed comparison against prior hallucination detection datasets applicable for HalDec. Our dataset includes more responses and includes text-to-image models as the evaluation target. In particular, it offers larger textual coverage, covering 1.6M words, 94k sentences, and a vocabulary of 17k unique word types, than prior datasets.

Image domain. Figure D illustrates the ratio of incorrect sentences on each image category in the CC12M. All Captioners tend to produce more errors in *Text* and *Illustration* domains, while they are relatively robust in real images. This can be because of the bias in the training data of the Captioners.

Error analysis w.r.t position of the sentence. In Fig. E, we present the ratio of incorrect sentences across sentence positions for each model. Among image captioning models, incorrect sentences tend to appear most frequently in the second to fourth positions. Interestingly, the very first sentence is less likely to contain hallucinations. This may be because the first sentence often serves as an overall image caption. In contrast, the second and subsequent sentences typically provide more detailed descriptions, which are more prone to errors. For positions beyond the sixth sentence, the error rate decreases again. These

	<p>Type: Object Captioner: Llama-4</p> <p>The image depicts a young girl with her mouth covered by a piece of tape, conveying a sense of silence or restraint.</p>		<p>Type: Attribute Captioner: LLaVA</p> <p>The bear's eyes are closed, adding to the sense of tranquility in the scene.</p>
	<p>Type: Number Captioner: CogVLM</p> <p>Four skiers are in the frame, each wearing distinctive skiing attire and numbers.</p>		<p>Type: Text Captioner: Qwen-2</p> <p>The primary focus is on a large, partially broken-down sign that reads "Don't Feed the Dead" in a distressed, scratchy font.</p>
	<p>Type: Relation Text2Image: GPT-Gen</p> <p>A steaming cup of tea rests delicately on the arm rest of the chair, sending wisps of fragrant vapor into the air.</p>		<p>Type: Location Text2Imag: SD</p> <p>In a serene meadow, an adorable alpaca stands on the left side of the image, gazing curiously towards the right.</p>
	<p>Type: Direction Captioner: GPT</p> <p>The bird is facing to the right, and its beak is in contact with a cluster of berries.</p>		<p>Type: Illusion Captioner: ShareGPT</p> <p>One of them is holding a towel, perhaps ready to wipe off the player's sweat after an intense rally.</p>

Figure C. Example annotations of error type. Hallucinations are highlighted in red.

Table C. Compared to existing hallucination detector benchmarks for image captions based on their evaluation split, AlignBench offers the largest number of responses, providing annotations for at least 1,000 responses per model across eight models. This scale enables detailed, model-wise performance analysis and facilitates a deeper understanding of detector characteristics. For datasets that are not publicly available or lack information, the corresponding statistics are reported as NA.

Dataset	Segment Annotation	# halluc. types	# models	# sentences	words/Sent.	# vocab.	# unique image	Sent. Generation
Foil [41]	✓	✗	0	5k	11.8	4.1k	2.5k	Rule-base
HAT [41]	✓	✗	1	0.4k	13.6	1.2k	0.4k	Captioner
ARO [61]	✓	✓	0	52k	7.6	1.5k	6.6k	Rule-base
Winoground [48]	✓	3	0	1.6k	9.0	0.9k	0.8k	Human
SugarCrepe [22]	✗	3	0	2k	11.1	2.2k	1.5k	Language Model
SeeTrue [58]	✓	✗	1	6.9k	11.5	1.5k	6.9k	T2I model
GenAI-Bench [31]	✗	6	10	1.6k	12.6	4.3k	9.6k	T2I model
MHalDetect [20]	✓	✗	1	14k	18.0	4.4k	0.8k	Captioner
HaELM [52]	✗	✗	3	1.5k	13.7	1.6k	NA	Captioner
MHaluBench [10]	✓	4	8	0.7k	14.6	1.3k	0.2k	Captioner + T2I
ZINA [51]	✓	6	12	NA	NA	NA	NA	Captioner
AlignBench (Ours)	✓	9	8	89k	17.7	42k	4k	Captioner + T2I

later sentences often serve as overall conclusions or closing remarks rather than detailed descriptions, which may make them similar to the first sentence and thus less prone to errors.

Analysis w.r.t hallucination types. Figure F describes the type of hallucinations we provide. Our dataset covers various kinds of hallucinations.

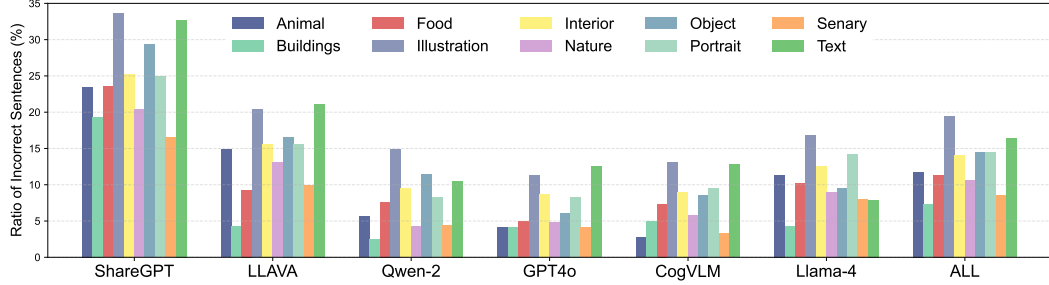


Figure D. **Ratio of incorrect sentences for each image domain.** All models tend to produce more errors in domains such as *illustration* and *Text*.

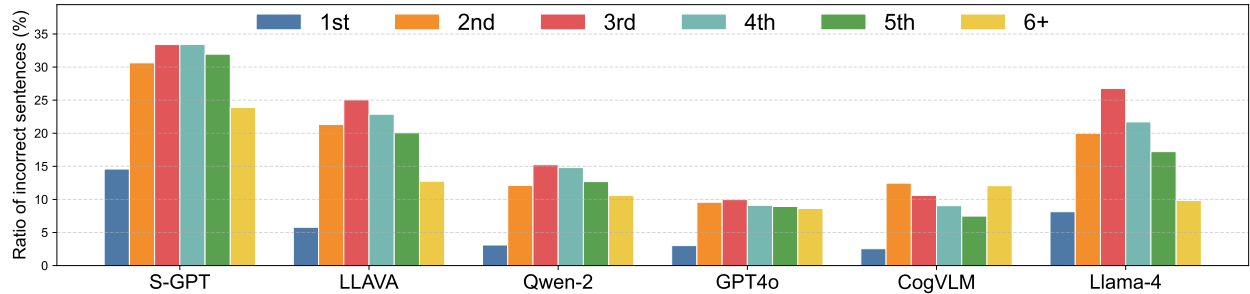


Figure E. **Ratio of incorrect sentences within each sentence position per model.** Different colors indicate different positions. All models produce fewer errors at the 1st position.

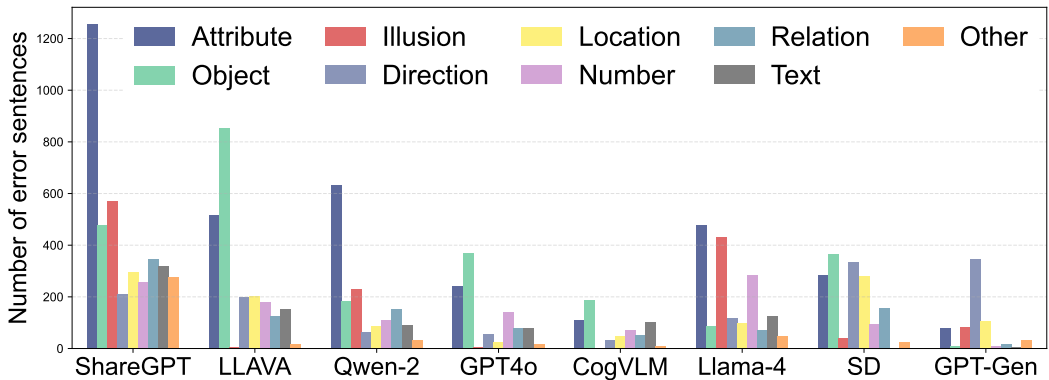


Figure F. **Number of hallucinations for each category.** Most models make many mistakes in attributes and text.

E. Details of Experimental Setups

E.1. Details of Evaluation

Source of models. We employ models available in HuggingFace and base our code on the HuggingFace Transformers package.

Computation. At most eight A100 80GB GPUs are used for inference of a single model.

Prompt. We employ the prompt below to compute the alignment score for decoder-based VLM.

Prompt to compute image-sentence alignment

You are given an image and a caption describing the given image. Your task is to judge if the caption describes the image correctly. If you think the sentence does not describe the image correctly, return low the score. If you think there is no mistake in the caption, return high score. Judge the correctness from 0-100 points. Return the output in the form of dictionary, e.g., “score”: 50. Please first output the correctness points before explaining the reason for the score.

Caption:

Similarly, we use the prompt below to obtain the results of the chain of thought.

Chain-of-thought prompt

You are given an image and a caption describing the given image. Your task is to judge if the caption describes the image correctly. If you think the sentence does not describe the image correctly, return low the score. If you think there is no mistake in the caption, return high score. Judge the correctness from 0-100 points. Return the output in the form of dictionary, e.g., “score”: 50. Please first explain the reason of scoring in ** two or three ** sentences and output the correctness points as shown above.

Caption:

Parsing. After obtaining the text output, we write a parser to convert the output into an integer. Models sometimes did not properly follow the prompt, and we could not parse such output. For such a sample, we assign 50 as its alignment score. In Table 3, we present models with their failure rate less than 5%. Also, the failure rate of a well-performing model is very low.

Annotation details in self-preference analysis. In Sec. 4.2, we additionally provide sentence-level hallucination existence labels for Qwen-2.5 (32B) and Gemma-3 (27B). To reduce the cost of annotation, we follow an annotation procedure different from the other 8 models, yet in a quality-ensured manner. Specifically, we randomly pick 500 images and generate captions using two models. Then, one quality-ensured annotator gives an annotation to 500 captions. This produces enough samples for analysis. We will include this split when publishing the dataset.

Prompt in hallucination localization. We employ the prompt below to obtain the results of hallucination localization.

Prompt for hallucination localization

You are given an image and a caption describing the given image. Your task is to localize the segment of the caption, which describes the image incorrectly. Please output the segment by marking the incorrect parts by **[]**, e.g., A **[red]** bird singing in a tree. Return the output in the form of a dictionary. Example format.

```
```json
{
 "output": "A **[red]** bird singing in a tree."
}
```
```

Caption:

Evaluation metric in hallucination localization. We evaluate the alignment between the word spans predicted by models and the ground-truth (GT) spans using an Intersection-over-Union (IoU) based criterion. Concretely, we compute the IoU between the predicted word range and the GT word range. In Table 5, a prediction is considered correct if its IoU with a GT span is greater than or equal to 0.3. Based on this criterion, we measure precision as the proportion of predicted spans that are judged correct.

F. Additional Experiments

Does incorporating the preceding sentences lead to improved performance? In our main paper, we focus on the evaluation of alignment between a single sentence and an image. This setting ignores the context from the preceding sentence in a caption since the model does not see the preceding sentences during inference. We study the effectiveness of adding the

Table D. Results of using preceding sentences as context.

| Detector | Context | S-GPT | Llava | CogVLM |
|----------------|---------|-------------|-------------|-------------|
| Llama-4 (109B) | ✓ | 80.7 | 78.6 | 77.2 |
| | | 80.6 | 79.1 | 73.5 |
| GPT5-mini | ✓ | 81.5 | 82.2 | 81.1 |
| | | 82.6 | 81.5 | 79.5 |

preceding sentences. Specifically, we feed all preceding sentences as well as the target sentence for evaluation as a prompt, *e.g.*, *a cat is running in a park. The cat is next to a kid. Think about the correctness of **The cat is next to a kid. ***. Table D compares the effect of adding contextual sentences. Surprisingly, we find that providing this additional context does not clearly improve image–text alignment. For Llama-4, adding context often degrades instruction following, leading to more frequent parsing errors. For GPT5-mini, no parsing errors are observed, but the performance still drops slightly. These results suggest that incorporating preceding sentences as context can interfere with judging the alignment between the target sentence and the image. Since not all language models excel at handling long sequences, evaluation on a single sentence can be fair in evaluating the image–text alignment ability.

Table E. Results of using Chain-of-Thought (COT).

| Detector | COT | Image-to-Caption Models | | | | | | Text-to-Image Models | |
|----------------|-----|-------------------------|--------------------|--------------------|--------------------|--------------------|--------------------|----------------------|--------------------|
| | | S-GPT | Llava | Qwen-2 | GPT4o | CogVLM | Llama-4 | SD | GPT-Gen |
| Llama-4 (109B) | ✓ | 80.7 | 78.6 | 77.6 | 67.5 | 77.2 | 59.9 | 81.1 | 64.7 |
| | | 80.6 (-0.1) | 80.8 (+2.2) | 80.0 (+2.4) | 71.1 (+3.6) | 80.1 (+2.9) | 62.4 (+2.5) | 80.8 (-0.3) | 65.1 (+0.4) |
| GPT4.1-mini | ✓ | 77.8 | 75.8 | 74.4 | 65.8 | 69.2 | 66.0 | 68.7 | 56.1 |
| | | 79.0 (+1.2) | 76.2 (+0.4) | 75.0 (+0.6) | 63.4 (-2.4) | 71.6 (+2.4) | 63.8 (-2.2) | 73.2 (+4.5) | 56.2 (+0.1) |

Chain-of-Thought improves the performance? Table E evaluates the impact of chain-of-thought reasoning [55], where detectors are prompted to generate a reasoning path before producing a score (see above for prompt details). For Llama-4, COT generally improves performance, whereas for some Captioners, the gains are marginal or even slightly negative. Results for GPT4.1-mini are mixed, wherein improvements highly depend on the evaluation target.

Table F. Ensembling detectors’ output improves performance in almost all cases. We highlight the increase or decrease from the *better* model used for ensembling next to each score.

| Detector | Num. of Ensemble | Image-to-Caption Models | | | | | | Text-to-Image Models | |
|---------------|------------------|-------------------------|--------------------|--------------------|--------------------|--------------------|--------------------|----------------------|--------------------|
| | | S-GPT | Llava | Qwen-2 | GPT4o | CogVLM | Llama-4 | SD | GPT-Gen |
| Llama-4-scout | 1 | 80.6 | 80.8 | 80.0 | 71.1 | 80.1 | 62.4 | 80.8 | 65.1 |
| Llama-4-scout | 5 | 83.2 (+2.6) | 83.0 (+2.2) | 81.8 (+1.9) | 74.4 (+3.4) | 82.2 (+2.1) | 65.1 (+2.7) | 83.0 (+2.2) | 65.9 (+0.8) |
| Llama-4-scout | 10 | 83.7 (+3.1) | 83.4 (+2.6) | 82.2 (+2.3) | 75.0 (+3.9) | 82.8 (+2.7) | 65.7 (+3.3) | 83.4 (+2.6) | 66.4 (+1.3) |

Self-ensemble improves performance. We further study the potential of ensembling. Unlike the analysis above, we ensemble outputs from a single model to refine detector’s score [14, 24]. To get different scores from a single model, we obtain different reasoning paths by stochastic sampling in the chain-of-thought. To ensure the diversity of COT, we set the temperature as 1.5 and top_p as 0.9. Table F presents the results in Llama-4, where the performance consistently improves in all Captioners. Also, using more ensemble paths tends to improve the performance, while the increase seems to saturate. Model ensembling can be an interesting direction to improve the performance in this task.

VLM detectors can surpass prior approaches. Table G presents the comparison to UniHD [10], which prompts LLM to utilize an open-vocabulary detector and OCR engine. The results indicate that advanced VLMs can surpass the approach without using such external tools. More detailed discussion is available in the appendix.

Mean intersection over union in hallucination localization. Table H shows the results of mean IoU in hallucinated segment localization. Specifically, we compute the intersection over union between the predicted and ground-truth segments and compute the average for all samples. Overall, the performance is consistent with what is reported in Table 5.

Additional results in self-preference evaluation. Fig. G illustrates self-preference score analysis for Gemma-27B, Llama-4, and Qwen2.5. Their self-preference tendency is significant, especially for Gemma-27B and Qwen2.5.

Table G. Comparison to existing HalDec approaches.

| Detector | GPT4o | SD |
|--------------|-------|------|
| UniHD [10] | 62.6 | 71.0 |
| Qwen-2.5 32B | 66.1 | 68.9 |
| Gemma-3 27B | 61.0 | 63.7 |
| Llama-4 109B | 67.7 | 81.1 |
| GPT-4.1-mini | 65.8 | 68.7 |

Table H. Mean IoU for hallucination localization task. Localizing the segment of the hallucinated caption remains difficult even for performant models.

| Detector | Params | Image-to-Caption Models | | | | | | Text-to-Image Models | | Avg. |
|--------------|--------|-------------------------|-------------|-------------|-------------|-------------|-------------|----------------------|-------------|-------------|
| | | S-GPT | Llava | Qwen-2 | GPT4o | CogVLM | Llama-4 | SD | GPT-Gen | |
| Qwen-2.5 | 32B | 13.8 | 15.1 | 11.7 | 15.1 | 16.0 | 10.7 | 11.4 | 9.4 | 12.9 |
| GPT-4.1-mini | - | 21.6 | 22.4 | 18.3 | 23.3 | 21.5 | 16.4 | 12.5 | 11.9 | 18.5 |
| Llama-4 | 109B | 22.6 | 20.8 | 22.7 | 26.4 | 23.2 | 17.3 | 10.7 | 9.0 | 19.1 |
| Llama-4 | 400B | 24.8 | 22.1 | 23.3 | 26.0 | 21.7 | 18.0 | 11.9 | 9.3 | 19.6 |

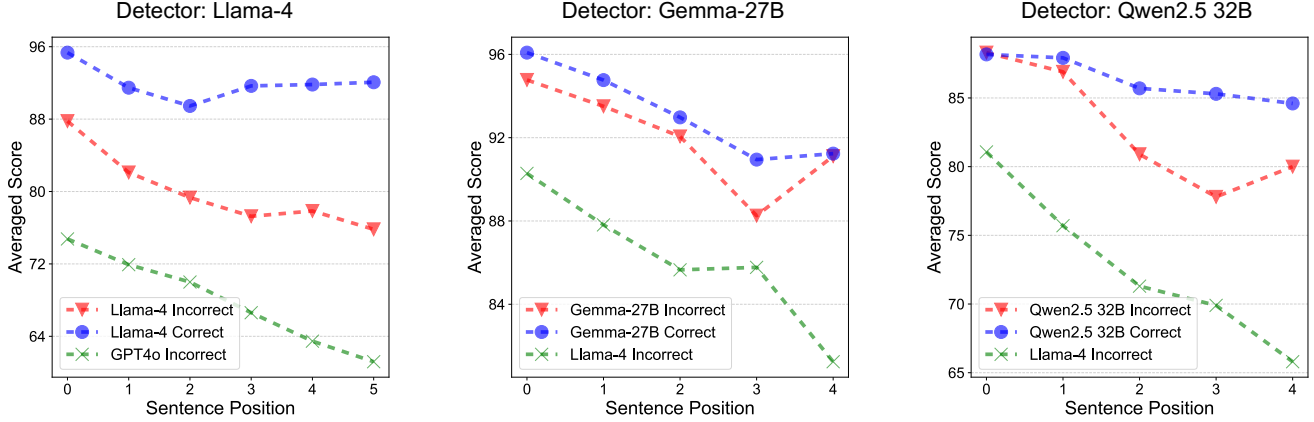


Figure G. Detector’s output score for their own output captions.

Distributions of evaluators’ outputs. Fig. H illustrates the distribution of evaluators’ scores for GPT-4o captions. Scores tend to concentrate on the points near 0 and 100 for Llama-4.

Additional examples of VLMs’ outputs. Figure I illustrates examples of input images, sentences, and corresponding correctness scores inferred by VLMs. VLMs tend to make errors in the location of the objects, the relationship between them, and small visual details.

G. Additional Examples of Annotations

We provide additional figures illustrating annotation results and representative hallucination cases: ShareGPT (Fig. J), LLaVA (Fig. K), Qwen-2 (Fig. M), GPT-4o (Fig. M), CogVLM (Fig. N), LLaMA-4 (Fig. O), Stable Diffusion (Fig. P), and GPT-Gen (Fig. Q).

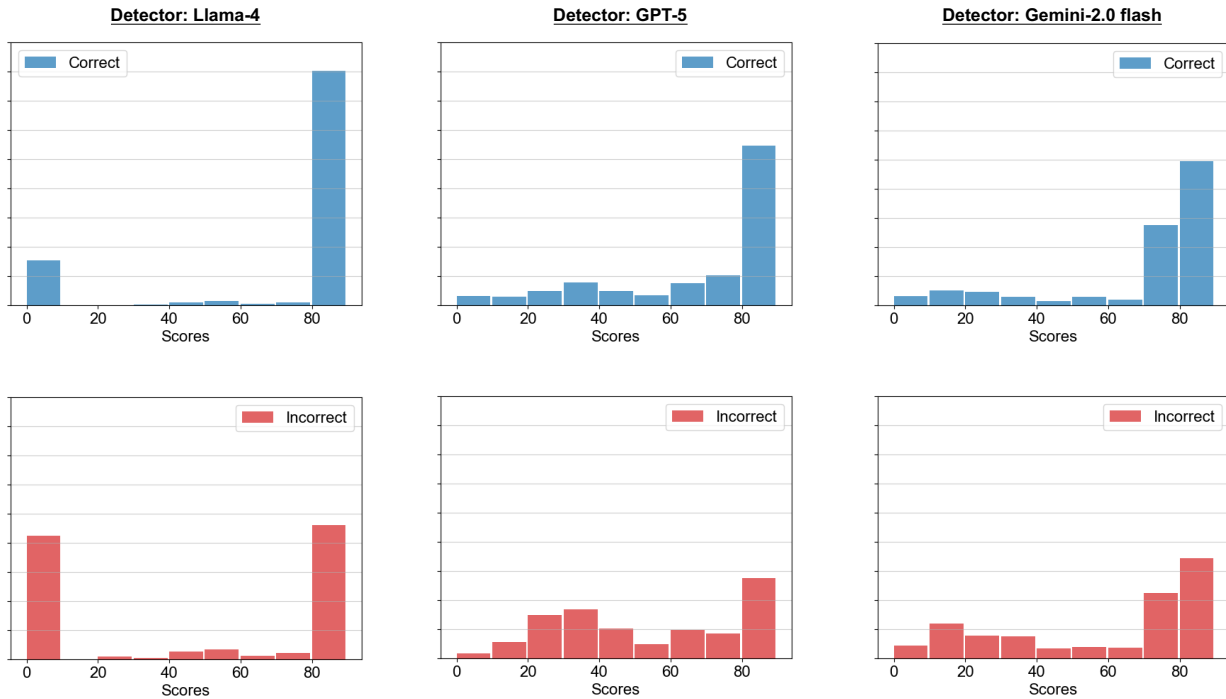


Figure H. **Distributions of evaluators' output scores.** We visualize the evaluators' scores for GPT-4o captions.

|  | <p>Captioner: LLaVA-Next</p> <p>In the image, a man is seen standing waist-deep in the ocean, holding a yellow surfboard.</p> <table border="1" data-bbox="393 502 752 551"> <thead> <tr> <th>Llama-4</th> <th>Gemma-27B</th> <th>GPT5o-mini</th> <th>Gemini</th> </tr> </thead> <tbody> <tr> <td>90</td> <td>95</td> <td>90</td> <td>100</td> </tr> </tbody> </table> | Llama-4 | Gemma-27B | GPT5o-mini | Gemini | 90 | 95 | 90 | 100 |  | <p>Text2Image: GPT4o</p> <p>In a serene forest clearing, a majestic doe stands at the center, her gentle gaze directed towards the soft rays of sunlight filtering through the trees above.</p> <table border="1" data-bbox="1078 502 1437 551"> <thead> <tr> <th>Llama-4</th> <th>Gemma-27B</th> <th>GPT5o</th> <th>Gemini</th> </tr> </thead> <tbody> <tr> <td>80</td> <td>95</td> <td>90</td> <td>100</td> </tr> </tbody> </table> | Llama-4 | Gemma-27B | GPT5o | Gemini | 80 | 95 | 90 | 100 |
|---|---|------------|-----------|------------|----------|-----|-----|----|-----|--|---|---------|-------------|------------|--------|----|-----|-----|-----|
| Llama-4 | Gemma-27B | GPT5o-mini | Gemini | | | | | | | | | | | | | | | | |
| 90 | 95 | 90 | 100 | | | | | | | | | | | | | | | | |
| Llama-4 | Gemma-27B | GPT5o | Gemini | | | | | | | | | | | | | | | | |
| 80 | 95 | 90 | 100 | | | | | | | | | | | | | | | | |
|  | <p>Captioner: ShareGPT</p> <p>The image presents a restaurant menu, neatly organized into two distinct sections</p> <table border="1" data-bbox="393 699 752 747"> <thead> <tr> <th>Llama-4</th> <th>Gemma-27B</th> <th>GPT5o-mini</th> <th>Gemini</th> </tr> </thead> <tbody> <tr> <td>0</td> <td>95</td> <td>10</td> <td>100</td> </tr> </tbody> </table> | Llama-4 | Gemma-27B | GPT5o-mini | Gemini | 0 | 95 | 10 | 100 |  | <p>Captioner: Qwen-2</p> <p>The image shows two identical silver candlesticks placed side by side.</p> <table border="1" data-bbox="1078 699 1437 747"> <thead> <tr> <th>Llama-4</th> <th>Gemma-27B</th> <th>GPT5o-mini</th> <th>Gemini</th> </tr> </thead> <tbody> <tr> <td>90</td> <td>90</td> <td>100</td> <td>10</td> </tr> </tbody> </table> | Llama-4 | Gemma-27B | GPT5o-mini | Gemini | 90 | 90 | 100 | 10 |
| Llama-4 | Gemma-27B | GPT5o-mini | Gemini | | | | | | | | | | | | | | | | |
| 0 | 95 | 10 | 100 | | | | | | | | | | | | | | | | |
| Llama-4 | Gemma-27B | GPT5o-mini | Gemini | | | | | | | | | | | | | | | | |
| 90 | 90 | 100 | 10 | | | | | | | | | | | | | | | | |
|  | <p>Text2Image: Stable Diffusion</p> <p>A cozy reading nook is at the top left corner of the room, where a thick, open book lies on a plush armchair</p> <table border="1" data-bbox="393 927 752 975"> <thead> <tr> <th>Llama-4</th> <th>Gemma-27B</th> <th>GPT5o-mini</th> <th>Gemini</th> </tr> </thead> <tbody> <tr> <td>40</td> <td>90</td> <td>90</td> <td>95</td> </tr> </tbody> </table> | Llama-4 | Gemma-27B | GPT5o-mini | Gemini | 40 | 90 | 90 | 95 |  | <p>Captioner: Llama-4</p> <p>The image presents a meticulously arranged display of Japanese sweets and a bottle of sake on two red lacquerware plates, set against a warm wooden table.</p> <table border="1" data-bbox="1078 927 1437 975"> <thead> <tr> <th>Llama-4</th> <th>InternVL2.5</th> <th>GPT5o-mini</th> <th>GPT5o</th> </tr> </thead> <tbody> <tr> <td>90</td> <td>95</td> <td>88</td> <td>60</td> </tr> </tbody> </table> | Llama-4 | InternVL2.5 | GPT5o-mini | GPT5o | 90 | 95 | 88 | 60 |
| Llama-4 | Gemma-27B | GPT5o-mini | Gemini | | | | | | | | | | | | | | | | |
| 40 | 90 | 90 | 95 | | | | | | | | | | | | | | | | |
| Llama-4 | InternVL2.5 | GPT5o-mini | GPT5o | | | | | | | | | | | | | | | | |
| 90 | 95 | 88 | 60 | | | | | | | | | | | | | | | | |
|  | <p>Captioner: LLaVA-Next</p> <p>○ In the image, the renowned actor Johnny Depp is the central figure.</p> <table border="1" data-bbox="393 1153 752 1201"> <thead> <tr> <th>Llama-4</th> <th>Gemma-27B</th> <th>GPT5o-mini</th> <th>Gemini</th> </tr> </thead> <tbody> <tr> <td>100</td> <td>100</td> <td>0</td> <td>100</td> </tr> </tbody> </table> | Llama-4 | Gemma-27B | GPT5o-mini | Gemini | 100 | 100 | 0 | 100 |  | <p>Captioner: GPT-4o</p> <p>○ The image shows a person snowshoeing in a snowy landscape.</p> <table border="1" data-bbox="1078 1153 1437 1201"> <thead> <tr> <th>Llama-4</th> <th>Gemma-27B</th> <th>GPT5o-mini</th> <th>Gemini</th> </tr> </thead> <tbody> <tr> <td>0</td> <td>100</td> <td>95</td> <td>100</td> </tr> </tbody> </table> | Llama-4 | Gemma-27B | GPT5o-mini | Gemini | 0 | 100 | 95 | 100 |
| Llama-4 | Gemma-27B | GPT5o-mini | Gemini | | | | | | | | | | | | | | | | |
| 100 | 100 | 0 | 100 | | | | | | | | | | | | | | | | |
| Llama-4 | Gemma-27B | GPT5o-mini | Gemini | | | | | | | | | | | | | | | | |
| 0 | 100 | 95 | 100 | | | | | | | | | | | | | | | | |
|  | <p>Captioner: ShareGPT</p> <p>○ In the center of the image, a group of teddy bears is captured in a moment of camaraderie.</p> <table border="1" data-bbox="393 1360 752 1408"> <thead> <tr> <th>Llama-4</th> <th>Gemma-27B</th> <th>GPT5o-mini</th> <th>Gemini</th> </tr> </thead> <tbody> <tr> <td>80</td> <td>90</td> <td>95</td> <td>15</td> </tr> </tbody> </table> | Llama-4 | Gemma-27B | GPT5o-mini | Gemini | 80 | 90 | 95 | 15 |  | <p>Captioner: Qwen-2</p> <p>○ The image shows a street scene with several notable elements</p> <table border="1" data-bbox="1078 1360 1437 1408"> <thead> <tr> <th>Llama-4</th> <th>Gemma-27B</th> <th>GPT5o-mini</th> <th>Gemini</th> </tr> </thead> <tbody> <tr> <td>90</td> <td>95</td> <td>10</td> <td>100</td> </tr> </tbody> </table> | Llama-4 | Gemma-27B | GPT5o-mini | Gemini | 90 | 95 | 10 | 100 |
| Llama-4 | Gemma-27B | GPT5o-mini | Gemini | | | | | | | | | | | | | | | | |
| 80 | 90 | 95 | 15 | | | | | | | | | | | | | | | | |
| Llama-4 | Gemma-27B | GPT5o-mini | Gemini | | | | | | | | | | | | | | | | |
| 90 | 95 | 10 | 100 | | | | | | | | | | | | | | | | |
|  | <p>Captioner: Llama-4</p> <p>○ The road is surrounded by a guardrail.</p> <table border="1" data-bbox="393 1560 752 1609"> <thead> <tr> <th>Llama-4</th> <th>Gemma-27B</th> <th>GPT5o</th> <th>Qwen-2.5</th> </tr> </thead> <tbody> <tr> <td>70</td> <td>20</td> <td>30</td> <td>70</td> </tr> </tbody> </table> | Llama-4 | Gemma-27B | GPT5o | Qwen-2.5 | 70 | 20 | 30 | 70 |  | <p>Text2Image: GPT4o</p> <p>○ In a vibrant, lush forest, a green salamander is perched on a moss-covered rock near the bottom left corner of the scene.</p> <table border="1" data-bbox="1078 1560 1437 1609"> <thead> <tr> <th>Llama-4</th> <th>Gemma-27B</th> <th>GPT5o</th> <th>Gemini</th> </tr> </thead> <tbody> <tr> <td>90</td> <td>90</td> <td>30</td> <td>100</td> </tr> </tbody> </table> | Llama-4 | Gemma-27B | GPT5o | Gemini | 90 | 90 | 30 | 100 |
| Llama-4 | Gemma-27B | GPT5o | Qwen-2.5 | | | | | | | | | | | | | | | | |
| 70 | 20 | 30 | 70 | | | | | | | | | | | | | | | | |
| Llama-4 | Gemma-27B | GPT5o | Gemini | | | | | | | | | | | | | | | | |
| 90 | 90 | 30 | 100 | | | | | | | | | | | | | | | | |

Figure I. Examples of input image and sentences with detectors' correctness scores. Higher scores indicate greater confidence in correctness. We highlight detectors' errors in red within the text.



The image captures a serene and inviting outdoor patio area.

The precise placement of objects and their relative positions contribute to the overall balance and harmony of the scene.

Dominating the scene is a large window that frames a picturesque view of a pool and lush greenery, offering a glimpse into the tranquility of the surroundings.

The window is framed by a sturdy brick wall, adding a rustic charm to the setting.

Number

In front of the window, **two** wicker chairs with vibrant floral cushions invite relaxation.

A potted plant rests on the floor next to the chairs, adding a touch of nature to the scene.

Attribute

On the right side of the image, a painting of a bird in **flight** brings a dynamic element to the otherwise static scene.

Attribute

The bird, captured **mid-flight**, adds a sense of movement and life to the composition.

Overall, the image presents a harmonious blend of man-made structures and natural elements, creating a space that is both functional and aesthetically pleasing.



In the center of a white background, there's a lively cartoon can of milk.

The entire scene is set against a stark white background, which puts the focus entirely on the can and its actions.

The image is simple yet engaging, with the can's actions and expressions adding a touch of whimsy and humor.

Illusion

The can, painted in hues of blue and white, is anthropomorphized with a pair of arms and **legs**.

It's not just any can, though.

This one has a face, complete with eyes, a nose, and a mouth, giving it a friendly and approachable demeanor.

Attribute

The can is actively engaged in an action—it's **holding up** a lightbulb above its head.

The lightbulb, a symbol of an idea or inspiration, is glowing brightly, indicating that the can has had a sudden thought or realization.

Illusion

Adding to the can's character, it's wearing a **hat**.

Illusion

The **hat** is brown, contrasting with the blue and white of the can.

Attribute

The word "MILK" is boldly written on the can in **black** letters, standing out against the blue and white background.



In the vast expanse of the clear blue sky, a vibrant kite dances in the wind.

The kite, a striking contrast of red and white, is adorned with black stripes that add a touch of elegance to its appearance.

Object

It's not just any ordinary kite, but one that bears the logo of a **bird**, perhaps symbolizing freedom and soaring heights.

The kite is tethered to the earth by four strings, two on each side, held firmly by unseen hands on the ground.

These strings, like lifelines, connect the kite to its earthly roots, ensuring it doesn't stray too far from home.

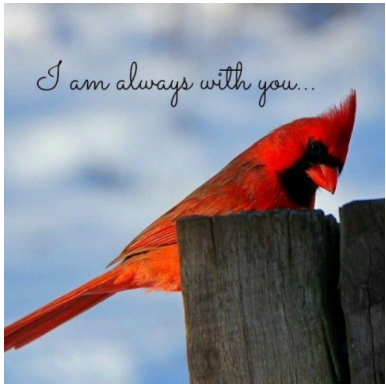
Location

The kite is positioned towards the top **right corner** of the image, as if it's eagerly reaching for the heavens.

Its position relative to the edges of the image suggests it's flying high above any potential obstructions.

This image captures a moment of joy and freedom, a snapshot of a kite's journey against the backdrop of an endless blue sky.

Figure J. Example annotations of Share-GPT.



The image captures a moment of tranquility in nature.

A cardinal, with its vibrant red plumage, is perched on a wooden fence post.

Direction

The cardinal's head is turned **to the left**, as if it's surveying its surroundings.

Object

The fence post, weathered and gray, provides a stark contrast to the cardinal's vivid color.

The background is a serene blue sky, lightly brushed with wispy clouds.

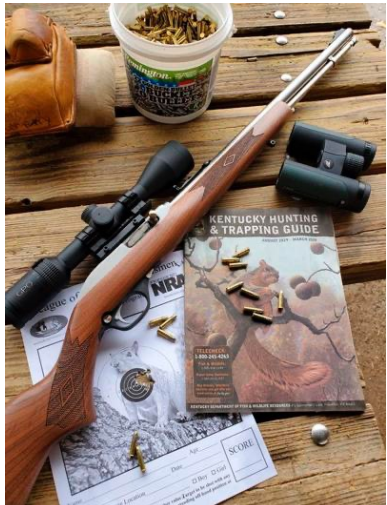
The sky's vastness adds a sense of depth to the image.

Overlaying this peaceful scene is a quote in a cursive font that reads, "I am always with you..."

Attribute

The quote, written in **white**, stands out against the blue background, adding a touch of sentimentality to the image.

The overall composition of the image suggests a harmonious blend of nature and human emotion.



The image shows a rifle with a scope mounted on a wooden surface, which appears to be a picnic table.

The overall setting suggests a hunting or shooting context, with the equipment laid out for use or display.

The image is taken during daylight, and the focus is sharp on the rifle and the immediate surrounding items, while the background is slightly blurred.

Direction

The rifle is positioned horizontally, with the barrel extending **towards the left side** of the frame.

To the right of the rifle, there is a pair of binoculars with a black body and a textured grip.

Text

In front of the binoculars, there is a container with a label that reads "**Buckshot**," indicating it contains shotgun pellets.

The container is open, and some of the pellets are visible.

On the left side of the rifle, there is a magazine with a label that reads "**NRA**," suggesting it is a publication from the National Rifle Association.

Below the magazine, there is a piece of paper with a target image and a score sheet, indicating that it might be used for target practice or competition.

The target has a bullseye and various scoring zones, and the score sheet has lines for recording the date, location, and scores.



In the center of the image, a wooden table is set with a meal.

On the left side of the table, there's a white plate holding a golden brown crepe, which is garnished with slices of banana.

Object

The crepe is accompanied by **a small bowl of red sauce**, adding a pop of color to the plate.

On the right side of the table, there's another white plate holding a colorful fruit salad.

Object

The salad is a vibrant mix of red watermelon, yellow pineapple, and **green kiwi**, all arranged neatly on the plate.

In the background, there's a white tiled floor that contrasts with the wooden table.

The floor extends into the distance, creating a sense of depth in the image.

The overall scene suggests a casual and inviting dining experience.

Figure K. Example annotations of LLaVA.



The image depicts a bronze sculpture of two individuals engaged in a conversation.

Object

One figure, appearing to be a **man**, is seated on a stone bench, while the other, likely a woman, stands beside him.

Both figures are dressed in vintage clothing, suggesting a historical or time-period-specific setting.

The bench is placed on a paved area, and there are bags placed at the feet of the figures.

Number

In the background, there are **three** people wearing modern clothing, standing and appearing to be engaged in a conversation or waiting.

The scene is set in a city environment, with a building and a partially open gate visible in the background.



The image shows a deep-dish pizza on a metal plate, with one slice **partially** removed.

The pizza has a thick crust and is topped with a generous amount of tomato sauce and cheese.

There is a spatula placed on the plate, likely used for serving.

Attribute

In the background, there is a person **holding** a glass of white wine.

The table appears to be made of dark wood, and there is a glass of water visible next to the wine glass.

The setting suggests a casual dining environment.



The image depicts a serene pastoral scene of three cows grazing in a lush green field.

Attribute

The foreground prominently features a brown cow with a **white** marking on its face, which is focused on grazing.

To the left, there is a black cow with distinctive white horns, also engaged in grazing.

Direction

In the background, partially obscured by the greenery, is another black cow, appearing to be standing and possibly looking in the **direction** of the camera.

The field is expansive, with the cows dispersed across the landscape, suggesting a peaceful and abundant grazing environment.

The background shows a mixture of trees and clear skies, adding to the natural beauty of the scene.

Figure L. Example annotations of Qwen-2.



The image depicts the interior of a bar with a group of people seated around a wooden bar counter.

Relation

The ceiling features a woven design, and a fan is mounted **above** the counter.

In the foreground, two men are sitting at the bar; one is holding a drink and appears to be smiling, while the other is holding a cigarette.

Object

Bottles and glasses are visible on the counter, along with various bar items like **bottle openers** and condiments.

Attribute

Further along the bar, two men and a **woman are engaged in conversation**, with one man wearing a sleeveless shirt and a hat.

The lighting is warm, giving the space a cozy ambiance.



The image features two individuals posing against a bright pink background decorated with small vinyl records and hanging spiral ribbons in red and orange.

The person on the left is wearing a green military-style helmet and holding a banana.

They are dressed in a suit with a dark tie and are wearing a bracelet on their wrist.

Object

The person on the right is wearing a black police helmet with an emblem on the front and **silver hoop earrings**.

They have short hair and are wearing a black top with a gray knitted shawl over it.

Direction

Both individuals are looking in the **same direction** with a slightly surprised or thoughtful expression.



The image shows two dogs and a cat lying on a bed.

The bedspread is light-colored with a quilt at the top.

The larger dog, with a tan coat, is lying diagonally across the bed.

The smaller dog, with a darker brindle coat, is curled up near the top left of the bed.

Relation

The cat, with a gray coat, is **nestled between them** on the quilt.

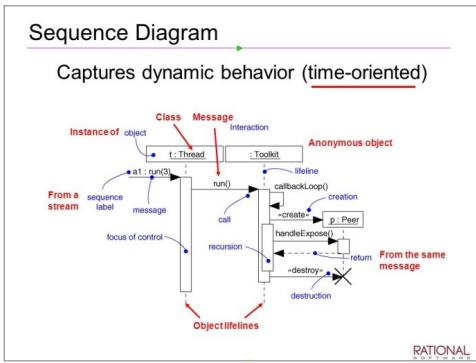
Attribute

There are two books on the bed, one with a visible cover and one with the cover **facing down**.

The visible book cover has an image and text, but the details are unclear from the image.

In the background, there is a nightstand with various items, and curtains cover the window behind the bed.

Figure M. Example annotations of GPT4o.



This image is a Sequence Diagram that illustrates the dynamic behavior of a time-oriented system.

Text

It shows interactions between different objects and classes, such as 'Instance of object', 'Class Message', 'Anonymous object', and '**Object lifetimes**'.

Illusion

The diagram uses various symbols like 'a1', '**a2**', '**b1**', '**b2**', and arrows to indicate the flow of messages and the sequence of events.



The image is a black and white photograph that captures an outdoor scene.

Text

In the foreground, there is a fire hydrant with the text 'MUELLER' and '**1914**' inscribed on it.

The hydrant is attached to a concrete base.

In the background, there is a wooden structure, possibly a deck or porch, with a person standing on it

Attribute

The person appears to be **looking out of a window or door**.

The surroundings include some trees, shrubs, and a rocky wall.



The image showcases a street scene in what appears to be an urban area.

Text

In the foreground, there is a white bus with the number '33' displayed on its front, heading towards '**Castro**'.

The bus has an advertisement on its side.

Attribute

To the left of the bus, there is a building with a **red** facade and a sign that reads 'BankofAmerica'.

The street is lined with trees, and in the background, there is a tall tower, possibly a communication or observation tower.

The sky is clear, suggesting a sunny day.

Figure N. Example annotations of CogVLM.



The image depicts a young woman in a boxing ring, wearing black and yellow boxing gloves.

The woman has long brown hair tied back in a ponytail and is dressed in a sleeveless top.

Attribute

She is positioned centrally in the frame, with her **right** arm extended forward, showcasing her glove.

Illusion

In the foreground, **another pair of boxing gloves** is visible, although they are out of focus.

The background features a blue floor and white ropes surrounding the ring, with windows on the left side that allow natural light to enter.

The overall atmosphere suggests that the woman is engaged in a training session or preparing for a fight, exuding a sense of determination and focus.



The image shows a cat lying on a bed in front of a bookshelf.

The cat is orange and white, with a white chest and paws, and an orange back and head.

Direction

It has pointy ears and appears to be looking **at the camera**.

The cat is lying on a bed with a yellow, green, blue, and white quilt or comforter.

The bed appears to have a white sheet or comforter underneath the quilt.

In the background, there is a brown wooden bookshelf filled with books of various colors and sizes.

Attribute

The books are arranged in rows, with some standing upright and others **lying flat**.

The wall behind the bookshelf is painted light blue.

The overall atmosphere of the image suggests a cozy and comfortable setting, possibly a bedroom or study.



The image depicts a cat walking behind a bicycle wheel, with the cat's body partially obscured by the wheel.

The cat is positioned on a light-colored hardwood floor, facing to the right.

It has a slender build and features a brown coat with black stripes, as well as a long tail.

In the foreground, the bicycle wheel is prominently displayed, showcasing its black tire and silver rim.

Text

The wheel is attached to a black fork with white text that reads **"Trekstar"** and other illegible words.

Illusion

To the left of the main wheel, **another bicycle wheel** is visible, featuring a blue rim and black tire.

The overall atmosphere of the image suggests that the cat is exploring its surroundings, possibly in a home or indoor setting.

Figure O. Example annotations of Llama-4.



Attribute

In a sunlit garden, a vibrant orange carrot is nestled in rich, dark soil on the left side of the image, **partially** exposed as if it is peeking out from the ground.

Direction

To its right, a curious rabbit with soft, white fur is intently **looking at the carrot**, its ears perked up in excitement.

In the background, blooming flowers sway gently in the breeze, their colors contrasting beautifully with the earthy tones of the soil.

Illusion

Above the scene, **a clear blue sky** adds to the serene atmosphere, casting gentle light over the garden.



Location

In a serene forest clearing bathed in early morning sunlight, a majestic moose stands proudly **on the right side** of the scene, its dark coat gleaming.

Attribute

It **lowers its head** to nibble on the lush greenery that sprawls at its hooves while keeping a vigilant gaze towards the left, scanning for any signs of movement.

Soft rays filter through the tall pines behind it, casting gentle shadows on the dried leaves covering the forest floor.

In the background, **flickers of a sparkling stream** reflect the sun's glow as it weaves through the trees.



Location

In a sunlit park **on the left side** of the scene, an old leather baseball glove rests on the grass, slightly worn from countless games.

Next to it, a new baseball gleams in the afternoon light, ready to be thrown but currently standing motionless.

Direction

In the background, a young boy in a bright baseball cap stands by a fence, **looking towards the glove** with eager anticipation in his eyes, wondering when he can play catch again.

Figure P. Example annotations of Stable Diffusion.



In a cozy children's bedroom, a fluffy teddy bear is nestled on the soft, cloud-patterned rug at the center of the room.

Direction

Its bright button eyes gaze thoughtfully **toward the window**, where soft rays of sunlight filter through pastel curtains, casting a warm glow around.

On the left side of the scene, a pile of colorful building blocks seems to spill out of a cheerful toy basket, while on the right, a collection of books rests neatly on a shelf, hinting at adventure awaits.

Attribute

The teddy bear, **slightly tilted**, watches over the joyful mess, embodying the protective whimsy of childhood.



Attribute

In a bright kitchen filled with the aroma of freshly baked cookies, a glowing microwave stands prominently on the countertop to the left, **its door slightly open** as if inviting a warm snack.

Attribute

A curious little cat with green eyes **sits on the floor** in front of it, gazing intently at the microwave's insides, waiting eagerly for the beep that announces its treat is ready.

A plate of colorful cupcakes sits on the table in the background, casting a soft shadow as sunlight filters through the window.

The wall above the microwave is adorned with recipe notes, adding a cozy, lived-in feel to the scene.



In the verdant wetlands of a sultry summer's afternoon, a crocodile lounge on a sundrenched, flattened rock at the right-hand side of the scene.

Direction

Its muscular body is soaked and dripping with water, remaining vigilant as it scans the shimmering pond that stretches outward in front of it.

Illusion

Surrounded by reeds and lily pads, its eyes glisten in the sunlight as it looks **towards tiny fish** darting happily beneath the surface, captivated by movement right below.

Meanwhile, colorful dragonflies flit high in the air, **casting fleeting shadows** on this eager predator's competent posture.

Figure Q. Example annotations of GPT-Gen.